CHARACTERIZATION AND SIMULATION OF RAINFALL-RUNOFF RELATIONS FOR HEADWATER BASINS IN WESTERN KING AND SNOHOMISH COUNTIES, WASHINGTON

By R.S. Dinicola

U.S. GEOLOGICAL SURVEY

Water-Resources Investigations Report 89-4052

Prepared in cooperation with the

KING COUNTY DEPARTMENT OF PUBLIC WORKS
KING COUNTY DEPARTMENT OF PLANNING AND COMMUNITY DEVELOPMENT
SNOHOMISH COUNTY DEPARTMENT OF PUBLIC WORKS
MUNICIPALITY OF METROPOLITAN SEATTLE

Tacoma, Washington
1990

DEPARTMENT OF THE INTERIOR

MANUEL LUJAN, JR., Secretary

U.S. GEOLOGICAL SURVEY

Dallas L. Peck, Director

For additional information write to:

District Chief
U.S. Geological Survey
1201 Pacific Ave., Suite 600
Tacoma, Washington 98402-4384

Copies of this report can be purchased from:

U.S. Geological Survey
Books and Open-File Reports Section
Federal Center, Bldg. 810
Denver, Colorado 80225

CONTENTS

ILLUSTRATIONS

TABLES

CONVERSION FACTORS

For the convenience of readers who may prefer to use metric (International System) units rather than the inch-pound units used in this report, values may be converted by using the following factors:

Multiply inch-pound unit	by	to obtain metric unit
inch (in.)	25.4	millimeter (mm)
foot (ft)	0.3048	meter (m)
acre	4,047	square meter (m^2)
	0.4047	hectare (ha)
square mile (mi^2)	259.0	hectare (ha)
	2.590	square kilometer (km^2)

Sea Level: In this report "sea level" refers to the National Geodetic Vertical Datum of 1929 (NGVD of 1929)--a geodetic datum derived from a general adjustment of the first-order level nets of both the United States and Canada, formerly called Sea Level Datum of 1929.

To convert degrees Fahrenheit (°F) to degrees Celsius (°C), use the following equation: $°C = 5/9\ (°F - 32)$.

CHARACTERIZATION AND SIMULATION OF RAINFALL-RUNOFF RELATIONS FOR HEADWATER BASINS IN WESTERN KING AND SNOHOMISH COUNTIES, WASHINGTON

By R.S. Dinicola

ABSTRACT

The characteristics of rainfall-runoff relations were hypothesized for the study area as a whole by using existing information. In undisturbed areas, shallow-subsurface flow from hillslopes mantled with glacial till, ground-water flow from glacial outwash deposits, and saturation overland flow from depressions, stream bottoms, and till-capped hilltops are the important runoff mechanisms. In disturbed, primarily urban areas, Horton overland flow, which is runoff generated from rain falling at a greater rate than the infiltration rate of the soil, is a significant mechanism, along with overland flow from impervious surfaces.

These hypothesized characteristics were incorporated into the Hydrologic Simulation Program-FORTRAN (HSPF) simulation model, and the model was calibrated concurrently at 21 stream-gage sites in the study area with hydrologic data from the 1985-86 water years. The calibration resulted in 12 sets of generalized HSPF parameters, one set for each land-segment type with a unique hydrologic response. The generalized parameters can be used with HSPF to simulate runoff from most headwater basins within the study area.

The average standard errors of estimate for calibrated streamflow simulation at all 21 sites were 7.9 percent for annual runoff, 11.2 percent for winter runoff, 13.1 percent for spring runoff, 40.1 percent for summer runoff, 21.7 percent for storm peak discharge, 21.4 percent for storm runoff volume, and 42.3 percent for all daily mean discharges. High flows were simulated more accurately than were low flows.

The simulation errors were not large enough to reject the hypothesized rainfall-runoff relations.

INTRODUCTION

Urbanization can alter the runoff characteristics of a drainage basin in many different ways (Savini and Kammerer, 1961), and construction of new residential communities and related commercial facilities is proceeding rapidly in the unincorporated areas of western King and Snohomish Counties, Washington. Local planners and engineers are committed to minimizing any adverse changes in runoff that may occur as a result of this urbanization. Planning for urban development on a drainage basin scale and predicting the potential hydrologic effects of this activity is one of their strategies for minimizing problems.

One of the standards that local regulatory agencies use for mitigating the effects of urban runoff is to limit post-development storm-runoff rates to the runoff rates expected for predevelopment conditions. Because most of the headwater drainage basins of interest have no stream discharge records, the pre- and post-development runoff rates are commonly estimated by using a rainfall-runoff hydrologic simulation model.

Many different types of rainfall-runoff hydrologic simulation models currently are in use. Regardless of the specific model used, it should be constructed to represent the spatial and temporal characteristics of rainfall-runoff relations in the study areas, and its performance should be validated within either the same study area, or at least in a physiographically and climatically similar area. This study was centered on those goals, and it was done in cooperation with the King County Department of Public Works, the King County Department of Planning and Community Development, the Snohomish County Department of Public Works, and the Municipality of Metropolitan Seattle (METRO).

Purpose and Scope

The purpose of this study is to characterize and simulate rainfall-runoff relations for headwater drainage basins in western King and Snohomish Counties, Washington. The purpose of this report is to present the hypothesized characteristics of the relations, and to describe the construction and calibration of a computer model designed to simulate the relations. Data collection for the study began in October 1984, and the part of the study described in this report was completed in September 1987.

Acknowledgments

Personnel from the King County Department of Public Works, the King County Department of Planning and Community Development, the Snohomish County Department of Public Works, and the Municipality of Metropolitan Seattle (METRO) have assisted with the design, data collection, and computer modeling involved in this study. They will also have primary responsibility for application of the results. A number of citizens from the counties have allowed gage installations on their property and have recorded data for the project. Their cooperation and assistance is appreciated.

Description of the Study Area

The study area is in the southeastern part of the Puget Sound Lowland in Washington State (fig. 1). The Lowland consists of a broad, rolling glacial-drift plain that merges eastward with foothills of the Cascade Range and is cut abruptly by six major alluvial valleys. The surface of the drift plain is covered mostly by deposits laid down about 15,000 years ago during the last period of glaciation in the area (Crandell and others, 1965). The drift plain is characterized by two common landform types: rolling, hilly glacial-till plains, and generally level glacial-outwash bench lands. Numerous lakes, swamps, and peat bogs occupy depressions on the till plains, whereas the outwash plains are generally well drained.

The five drainage basins selected for data collection cover about 260 mi^2 (square miles) in the 1,200-square-mile area of the drift plain in western King and Snohomish Counties. All the study basins are located on the drift plain. The major alluvial valleys along the Green, Cedar, Sammamish, Snoqualmie, Skykomish, and Snohomish Rivers are not included in the study area.

Most soils on the drift plain have formed in the deposits of glacial till and outwash. The till layer consists of 5 to 100 feet of dense basal, or lodgement, till (sediments laid down under the pressure of overlying ice) covered by a 3-foot-thick mantle of ablation till (sediments that settled from the surface of melting ice). The till is commonly exposed at the surface in the headwater areas of drainage basins, but it is usually buried beneath outwash deposits or has been completely eroded away in the valley bottoms. Highly permeable gravelly loam soils have formed in the loose ablation till, but the basal till remains mostly intact as an underlying layer of low permeability (locally referred to as 'hardpan'). The outwash (fluvial sediments deposited beyond the receding terminus of the ice) consists of unconsolidated deposits of gravel and sand that are 4 to 100 feet thick. Highly permeable gravelly loam soils, underlain by a highly permeable substratum, have formed in these deposits. Smaller areas of poorly drained soils occur at places on the study area. These soils have formed in the depressions on the till plains and in recently deposited alluvium in valley bottoms.

The climate of the region is of the midlatitude, west-coast-marine type, characterized by warm, dry summers, and cool, wet winters. The mean annual temperature in the region is about 51 °F, and the mean monthly temperatures in January and July are about 39 °F and 65 °F, respectively (U.S. Department of Commerce, 1982). Mean annual precipitation ranges from about 35 to 50 inches, and most of it falls as rain (U.S. Weather Bureau, 1965). Seventy to 80 percent of the precipitation falls from October through May during long-duration, light-to moderate-intensity storms. The relatively long wet season and growing season are conducive to lush vegetation. Evergreen forests and thick undergrowth blanket most of the study region. Potential evapotranspiration (PET) in the region averages about 25 inches annually, and actual evapotranspiration (ET) averages about 18 to 20 inches. A soil-moisture deficit generally occurs in July and August.

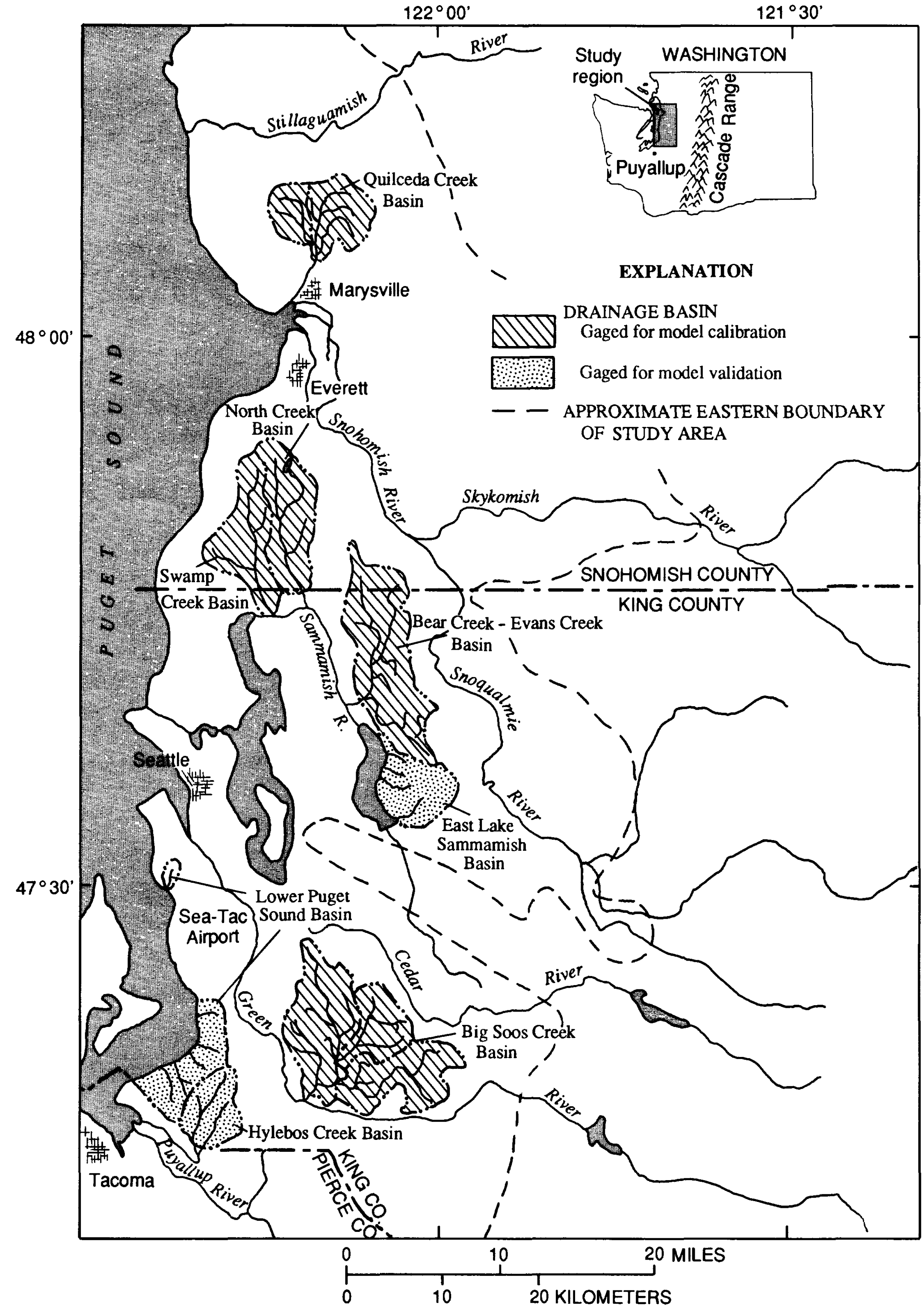

Figure 1.--Location of study region and basins used for model calibration and validation.

METHODS OF STUDY

A quantitative understanding of how a drainage basin responds to precipitation has proved to be elusive because of the complexity of the runoff processes involved and the spatial and temporal variability of precipitation and basin characteristics. A usual approach to understanding has been to incorporate available knowledge about the processes into a conceptual model of the system, and then to compare model-simulated results with observed data, such as streamflow. With regard to standard scientific method, wherein hypotheses are tested with measurements taken from carefully formulated, controlled situations, this approach is difficult.

Hydrologic fluxes measured in the field, such as streamflow, are usually basin-integrated responses, which do not often lead to clear understanding of all the individual processes involved in generating the flux. Additionally, many parameters in conceptual models cannot be measured independently in the field, but need to be calibrated with the same data collected to test the models. Regardless of these difficulties, simulation models of basin response remain the only practical approach to make comparisons between runoff theory and observations. The following methods were used to overcome some of the limitations of this approach.

The methods used for this study included formulation of hypotheses concerning rainfall-runoff relations in the study area, construction and calibration of the simulation model, and validation of the simulation model and the hypothesized rainfall-runoff relations.

Formulation of Hypotheses on Rainfall-Runoff Relations

The hypotheses concerning the character of rainfall-runoff relations in the study area were formulated using information from published literature. Previously tested runoff-generation theories were reviewed and analyzed with respect to the climate, physiography, and land use in the study area. The hypotheses were stated in general terms, applicable to the study area as a whole rather than for any one specific drainage basin.

Description of the Simulation Model

The computer simulation model used to test these hypotheses was the Hydrologic Simulation Program-FORTRAN (HSPF; U.S. Environmental Protection Agency, 1984). It was selected for use in this study primarily because (1) it can represent the hydrologic response to rainfall resulting from a number of physical processes, including those hypothesized to be important in this study area; (2) it simulates these responses continuously over time, rather than just during storms; and (3) it is capable of simulating the hydraulics of the complex natural and man-made drainage networks found in the study area.

The HSPF model incorporates a continuous water balance by tracking precipitation through a conceptual hydrologic system of a drainage basin. Ground-water recharge and discharge, shallow subsurface flow (interflow), and overland flow are simulated, lagged, and combined as discharge into a drainage network. The HSPF model does not simulate all of the relevant physical processes in a rigorous scientific manner, but rather represents those processes conceptually by using a series of interdependent nonlinear reservoirs. The outflows from these reservoirs are routed through the drainage network using a modified kinematic-wave mathematical algorithm. Any water conveyance system with known and unchanging hydraulic characteristics can be included in the network. This includes all streams, lakes, wetlands, culverts, and pipes, where variable backwater conditions do not normally occur.

Rainfall-runoff simulation with HSPF requires continuous records of precipitation and estimates of potential evapotranspiration (PET) to drive the model. Two general types of model parameters--physical-process-related and fixed--are used to represent the hydrologic features and the physical characteristics of a drainage basin. Process-related model parameters represent the amount of precipitation intercepted by structures or vegetation, the amount of water ponded on the surface or absorbed by forest litter, the amount of water stored in the soil, the soil-infiltration rate, the evapotranspiration rate, and the rates at which overland flow, interflow, and ground-water flow drain from the land to the stream channel system.

The names of the process-related HSPF parameters and what they are intended to represent are as follows:

CEPSC - Interception storage capacity of plants.
RETSC - Retention storage capacity of impervious areas.
UZSN - Upper-zone nominal storage. An index to the amount of depression and surface layer storage of a pervious area.
LZSN - Lower-zone nominal storage. An index to the soil moisture holding capacity.
INFILT - Infiltration capacity. An index to the infiltration capacity at the soil surface, and an indirect index of the percolation rate from the bottom of soil zone.
INTFW - Interflow index. In combination with INFILT, an index to the amount of water that infiltrates and flows as shallow subsurface runoff.
INFEXP - Infiltration equation exponent. Controls the rate at which infiltration decreases with increasing soil moisture.
INFILD - Ratio of the maximum to mean infiltration rate of a pervious area. Accounts for the degree of variations in the infiltration capacity.
LZETP - Lower-zone ET. An index to the density of deep-rooted vegetation on a pervious area.
BASETP - Fraction of available-PET demand that can be met with ground-water outflow. Simulates ET from riparian vegetation.
AGWETP - Fraction of available-PET demand that can be met with stored ground water. Simulates ET from phreatophytes in general.
LSUR - Average length of the overland flow plane.
SLSUR - Average slope of the overland flow plane.
NSUR - Average roughness of the overland flow plane.

IRC - Interflow recession parameter. An index of the rate at which shallow subsurface flow drains from the land.

AGWRC - Ground-water recession parameter. An index of the rate at which ground water drains from the land.

KVARY - Ground-water outflow modifier. An index of how much influence recent recharge has on ground-water outflow.

DEEPFR - Fraction of ground water that does not discharge to the surface within the boundaries of the modeled area.

Few of the process-related parameters have easily measurable physical analogs, so they are first estimated from available physiographic data and from the results of previous modeling studies, and then refined through calibration.

Fixed model parameters represent the areal extent of certain soil types, the amount of impervious area, the hydraulic characteristics of the drainage network, and other measurable features of a drainage basin. These parameters do have measurable physical analogs, so they remain unchanged during model calibration. They can be modified when different basin conditions, such as urbanization, are to be represented during an engineering application of the model.

Construction of the Simulation Model

The hypothesized rainfall-runoff characteristics were incorporated into the HSPF framework by using a distributed-parameter approach. This approach required division of a drainage basin into land segments, each with relatively uniform physical and hydrologic characteristics (Leavesley and others, 1983). All the area of a particular land segment need not be contiguous, so it was possible to represent complex mosaics of soil types, vegetative cover, topography, and land use by using a relatively few number of segments. Because characterization and simulation of generalized rainfall-runoff relations was the objective of this study, it was necessary to delineate enough land segments to represent all of the major physical and hydrologic characteristics found throughout the entire study area.

The goal of the segmentation scheme was to construct a conceptual model with the minimum number of land segments needed to simulate the physical and hydrologic processes of any upland drainage basin in the study area. This, in turn, reduced the number of parameters that required calibration, and led to a more realistic portrayal of the hypothesized processes that could be adequately tested with observed streamflow data.

Calibration of the Simulation Model

As previously mentioned, most of the process-related parameters in the simulation model have no measurable physical analogs, so they must be determined through calibration to observed data. The following data were collected in support of the calibration effort.

Five drainage basins--Quilceda Creek basin, North Creek basin, Swamp Creek basin, Bear Creek-Evans Creek basin, and Big Soos Creek basin--were gaged for model calibration (figs. 2-7). They were selected for study because they have soil, geologic, topographic, and land-use characteristics typical of the study area as a whole. Rainfall accumulation data were collected continuously at 15-minute intervals during the 1985-86 water years (a period of 12 consecutive months starting on October 1 of a year and ending September 30 of the following year) at 12 sites within these five basins (figs. 2-7). The density of rain-gage locations was about one gage per 10 mi^2 in all basins. Pan-evaporation data for March through October were obtained from the National Weather Service Class A evaporation pan site near Puyallup, Washington. Data from the pan were adjusted by a pan coefficient of 0.75 to represent PET (Farnsworth and Thompson, 1982). PET data for November through February were estimated by using a version of the Jensen-Haise equations (Bauer and Vaccaro, 1986). Temperature data from the National Weather Service station at the Seattle-Tacoma International Airport (SEATAC) were used in the Jensen-Haise PET calculations. The PET data were not adjusted across the study area because the mean annual temperature in the area varies only by about 1 $^{\circ}F$ (U.S. Department of Commerce, 1982).

Streamflow data were collected continuously at 15-minute intervals during the 1985-86 water years at 21 sites in the 5 basins gaged for model calibration (figs. 2-7). The gaged areas ranged from 1.28 to 65.8 mi^2. Additionally, estimates of instantaneous peak discharge were made a few times each year at 26 crest-stage gage sites throughout the study basins (figs. 2-7). Stage data were also collected about once weekly at 20 lakes and perennial wetlands in the basins. The streamflow data obtained for calibration of process-related parameters in the five basins are published elsewhere (U.S. Geological Survey, 1988).

In general, the objective of the calibration process was to do an initial test of the validity of the rainfall-runoff hypotheses over the study area as a whole. The hypotheses were incorporated into the simulation model by use of distributed land segments, each with its own postulated unique hydrologic response. During the calibration process, the condition was imposed that the set of process-related parameters used to simulate one type of land segment had to be numerically the same in all calibration basins where that particular land segment was present. The result of imposing this condition is that if the simulation model could be adequately calibrated within the constraints of the defined land segments, then the hypothesized rainfall-runoff relations underlying the segmentation scheme could be accepted conditionally, subject to further validation. Conversely, if the simulation model could not be adequately calibrated, then the hypothesized relations were rejected.

The more specific goal of model calibration was to adjust the process-related HSPF parameters so that streamflow simulated at the 21 gage sites closely matched observed streamflow from those sites. This involved doing a series of trial and error adjustments of the parameters while trying to minimize the errors between simulated and observed streamflow data. A computerized optimization routine was not available for this calibration of the HSPF model, and it was outside the scope of this project to develop such a routine. However, manual optimization was performed by minimizing a number of different statistics describing various attributes of the simulation errors.

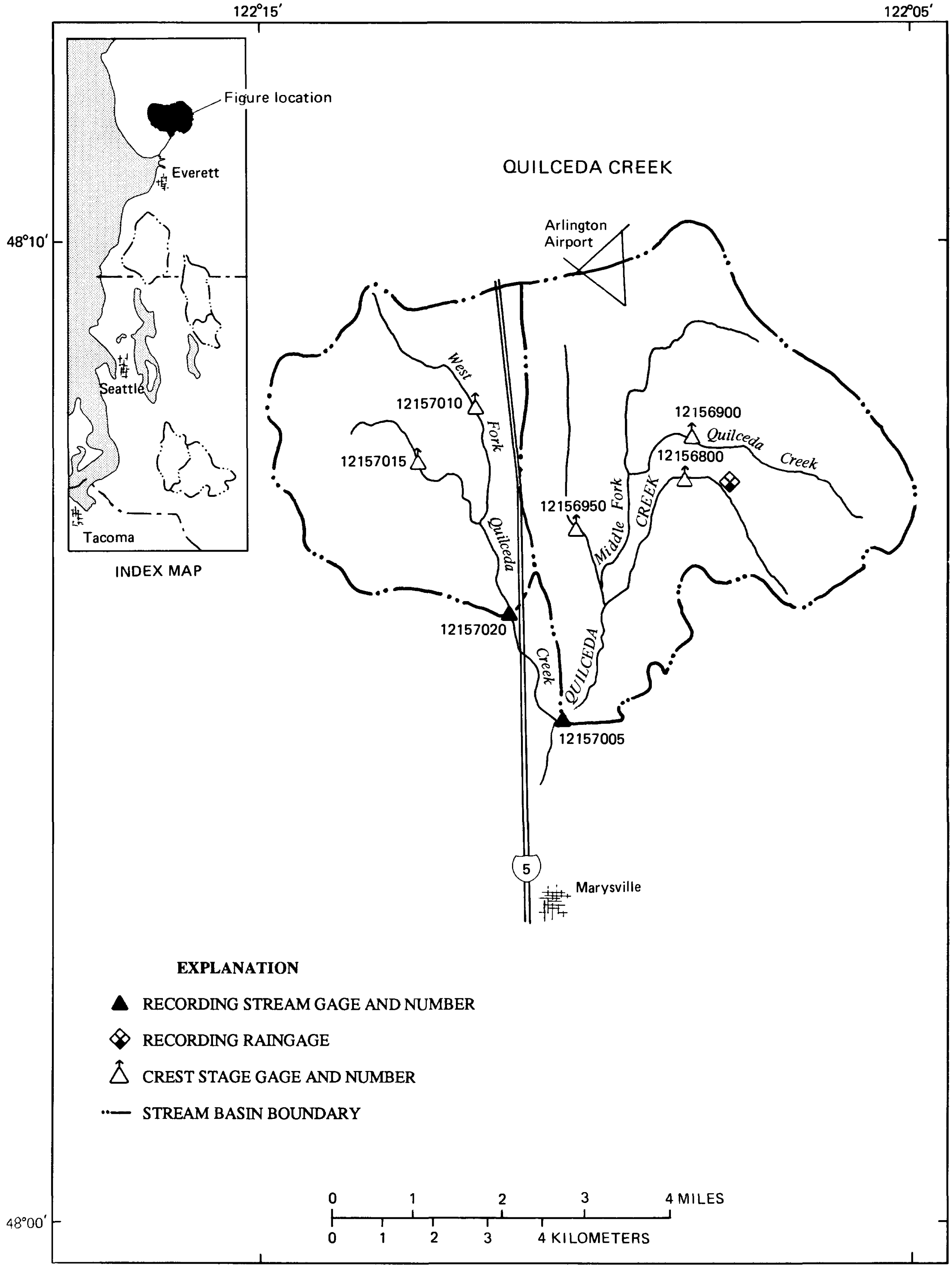

Figure 2.--Data-collection network for Quilceda Creek basin.

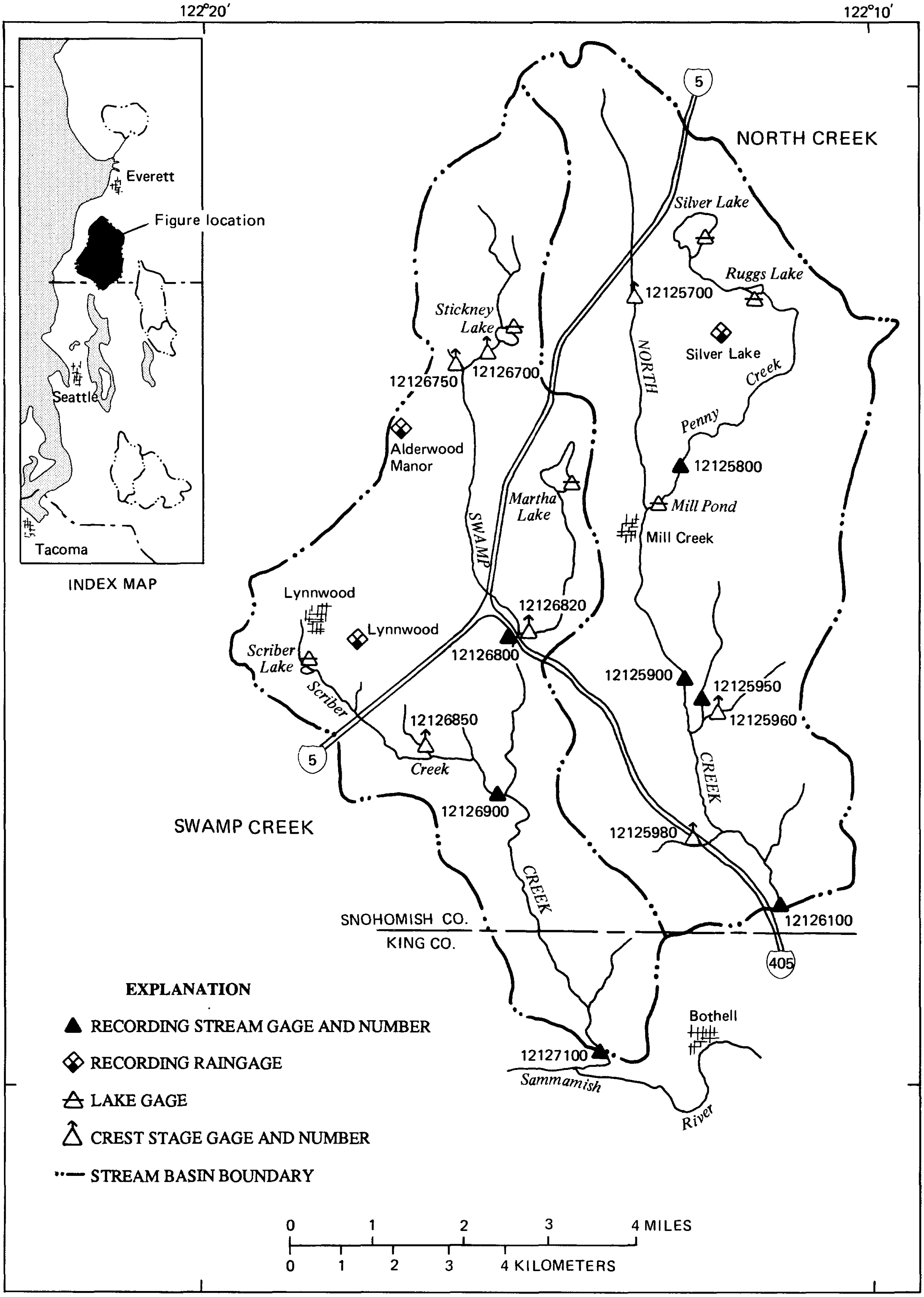

Figure 3.--Data-collection network for North and Swamp Creek basins.

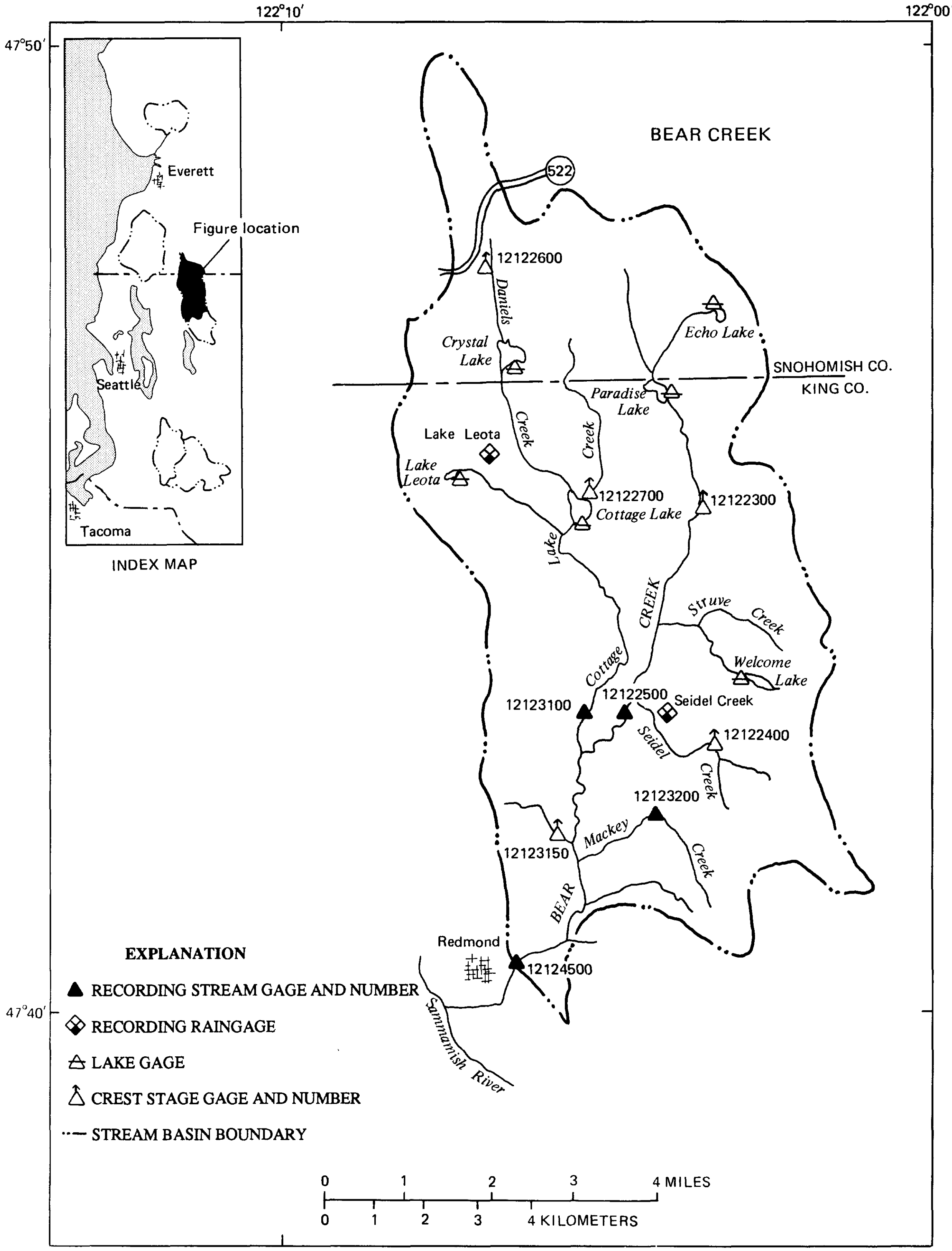

Figure 4.--Data-collection network for Bear Creek basin.

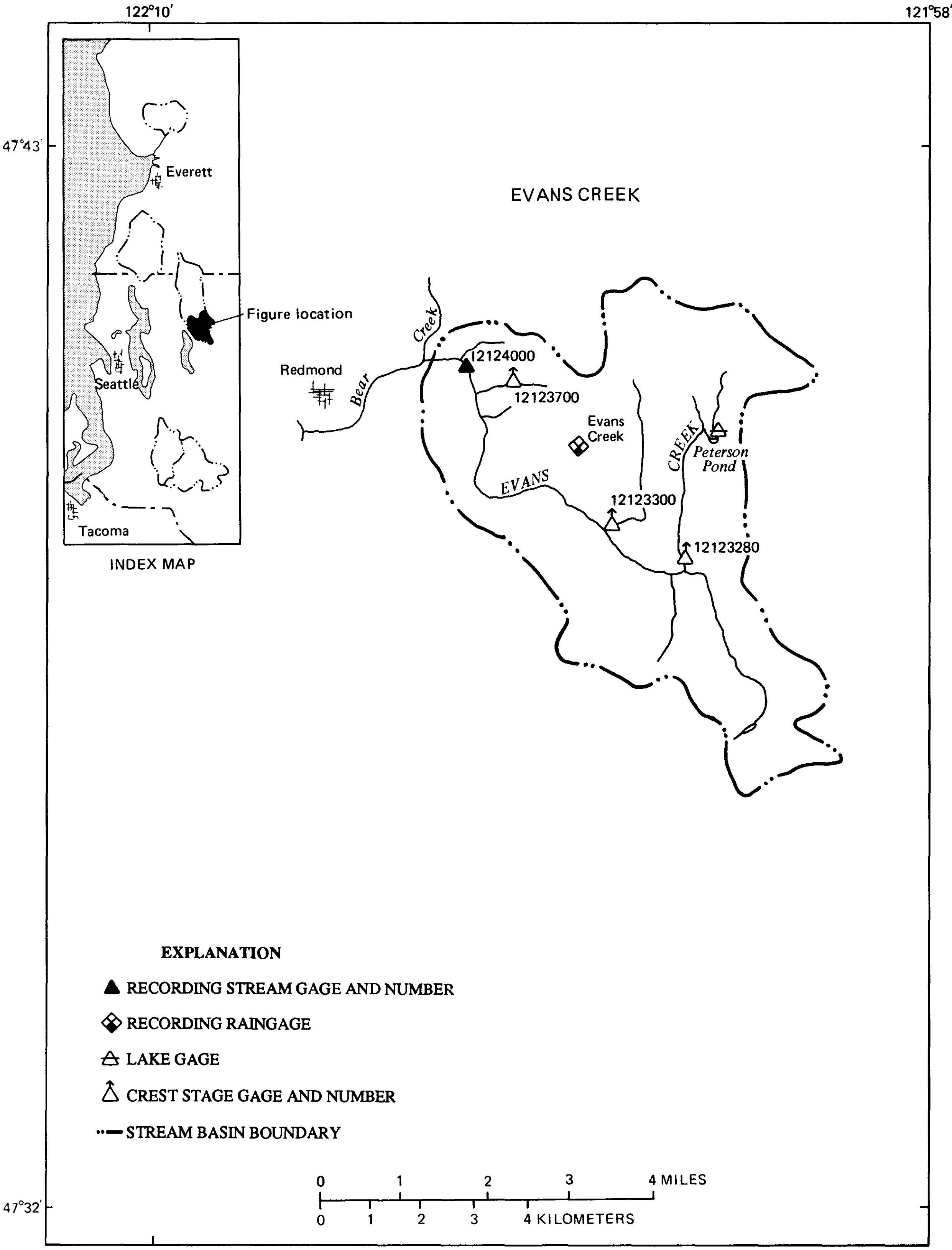

Figure 5.--Data-collection network for Evans Creek basin (tributary to Bear Creek).

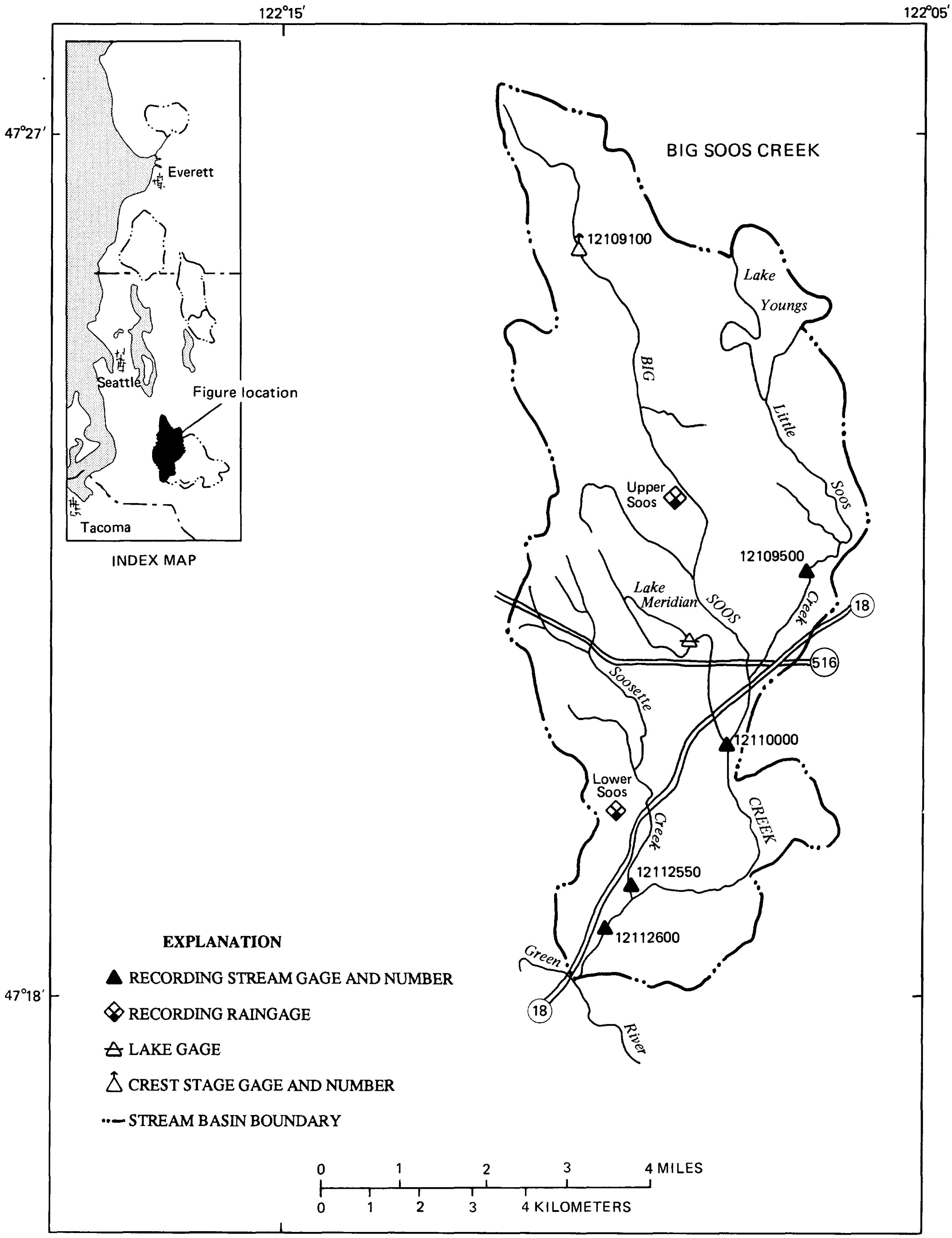

Figure 6.--Data-collection network for Big Soos Creek basin.

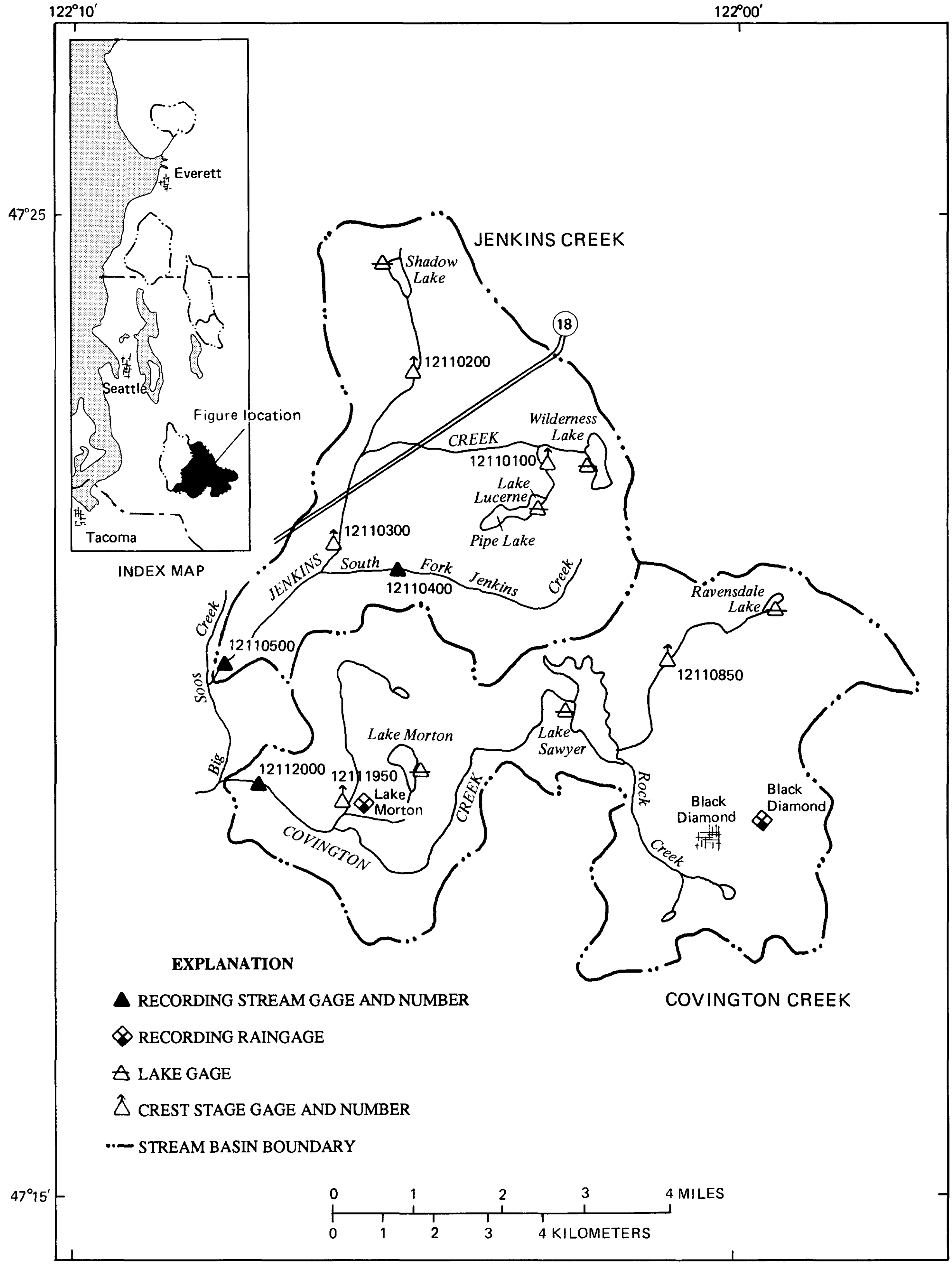

Figure 7.--Data-collection network for Jenkins Creek and Covington Creek basins (tributary to Big Soos Creek).

The HSPF model was calibrated concurrently for all 21 stream-gage sites in order to determine regionally consistent process-related parameters. As stated in the imposed condition, a given set of parameters characterizing a given type of land segment were held constant for each trial calibration in all basins where that segment existed, and subsequent adjustments of the parameters were likewise made consistently in all basins.

Validation of the Simulation Model

A proxy-basin test of the simulation model, and hence the rainfall-runoff relations incorporated therein, was designed to circumvent the dilemma that the model was both calibrated and initially tested with the same data sets. The proxy-basin test involves collecting streamflow and rainfall data from three other drainage basins physiographically similar to those used for model calibration, applying the previously calibrated simulation model to 12 additional stream-gage sites in these basins, and then comparing the simulated and observed streamflow data for the new basins.

Time series of precipitation, PET, and streamflow were obtained during the 1987-88 water years in three additional basins--Lower Puget Sound, Hylebos Creek, and East Lake Sammamish--to provide data for this validation effort (fig. 1). These basins are also representative of the characteristics found throughout the study area as a whole. Precipitation data were collected at 8 sites and streamflow data were collected at 12 sites in these basins. Estimates of PET were obtained as described for the basins used for calibration. Estimates of instantaneous peak discharge and observations of lake stage were also obtained at 27 sites and 21 lakes, respectively, in these basins. The validation part of this study is currently (1989) under way.

CHARACTERIZATION OF RAINFALL-RUNOFF RELATIONS

In characterizing rainfall-runoff relations, it is useful to examine separately the mechanisms that generate runoff from the undisturbed parts and from the disturbed, or developed, parts of the study area. Combined, these mechanisms control the rainfall-runoff relations of the study area as a whole, and a clear understanding of them is needed for successful hydrologic prediction.

In the undisturbed parts of the study area, four generally accepted mechanisms may generate runoff from rainfall (Pearce and others, 1986). These mechanisms are called Horton overland flow, subsurface flow, ground-water flow, and saturation overland flow. The physiographic and climatic characteristics of the study area determine which mechanism occurs in different settings.

Horton overland flow is generated from rain falling at a rate greater than the infiltration rate of a soil. It is the classical theory of runoff, wherein soils become saturated from the top downward. The 2-year, 1-hour rainfall intensity that falls on the study area is about 0.4 inches per hour, and the 100-year, 1-hour intensity is about 1.0 inch per hour (U.S. Department of Commerce, 1973). These rates are well below the saturated hydraulic conductivities of 2 to 6 inches per hour that are attributed to the soils that cover most of the study area (U.S. Department of Agriculture, 1973; 1983). Saturated hydraulic conductivity could be considered the minimum infiltration rate expected of a soil (Snider and Miller, 1985), so it is unlikely that Horton overland flow is an important runoff mechanism in the undisturbed part of the study area.

Subsurface flow is generated from rapid infiltration of rainwater and subsequent shallow-subsurface transmission of this water. This mechanism is commonly associated with hillslopes underlain by nearly impermeable substratum and covered with shallow, highly permeable soils. About two-thirds of the study area is underlain by basal till with a saturated hydraulic conductivity less than 0.06 inch per hour, covered by 30-inch-deep soils with saturated hydraulic conductivities of at least 2.0 inches per hour (U.S. Department of Agriculture, 1973; 1983). Transmission of subsurface flow is directly proportional to the angle of the slope, but rates of transmission in the study area are probably much slower than any type of overland flow, even on the steepest slopes. However, because the subsurface water most likely flows within the shallow soil profile, any decrease in slope or topographic convergence of slopes can cause this water to exfiltrate to the surface. Once it is on the surface, flow rates may increase by a factor of 100 to 500 (Dunne and Black, 1970). The subsurface flow mechanism is most likely an important control of rainfall-runoff relations in the undisturbed till parts of the study area.

Ground-water flow is generated from infiltration of rainwater and subsequent transmission of this water along typical ground-water flow paths. About 15 percent of the study area has the soils and substratum favorable to rapid infiltration: permeable soils underlain by even more permeable glacial outwash deposits. Transmission rates of ground water are proportional to the slope of the water table, but both the land surface and water table in glacial outwash deposits are usually only mildly sloping. As a result, transmission of ground water in the outwash deposits of the study area is slow and attenuated compared to other flow mechanisms. This slow runoff rate alone makes ground-water flow an important control of rainfall-runoff relations in the undisturbed outwash parts of the study area.

Saturation overland flow is generated from rain falling on saturated parts of a drainage basin near stream bottoms, depressions, or other flat or low-lying areas. The soils in these areas become saturated from the bottom up due to rising water tables. The water tables may be perched or apparent, and they are fed by direct precipitation onto a poorly drained area and perhaps by subsurface and ground-water flow from nearby hillslopes, also. This mechanism can be important in two slightly different settings in the study area. The first is the mildly undulating hilltop areas underlain by basal till. Such areas cover about 10 percent of the total study area. Downward percolation of soil water is limited by the nearly impermeable substratum, and lateral subsurface drainage is limited by gentle slopes. Infiltrated water can accumulate in many places within these areas and saturate the soil. Most of the water comes from direct precipitation, with smaller amounts coming in as subsurface flow from the surrounding low-gradient slopes.

Saturation will not occur from a single storm in these areas, because the soil profiles can store about 12 inches of water before saturation. However, after a series of storms, this slowly drained storage capacity may be overtopped.

The second saturation overland flow setting is in the larger topographic depressions and along drainage courses where the rising water tables are fed by direct infiltration and by substantial amounts of subsurface and (or) ground-water flow. Such areas cover another 10 percent of the entire study area. These areas can generate runoff more often than the hilltop areas, and some of these areas may remain saturated throughout the year. Saturation overland flow moves quickly in either setting, and is another important control of rainfall-runoff relations in the study area.

The runoff mechanisms previously described for undisturbed areas can be considerably altered by urban development, and new mechanisms become important. The most obvious is rapid, direct overland flow from impervious surfaces. More subtle changes can occur in impacted developed areas that are not actually covered with impervious surfaces.

Clearing and grading operations can compact soils and otherwise alter the structure of the soils. Also, fine-grained topsoils are commonly applied to the ground surface in lawns, parks, and golf courses, and deep-rooted trees are often replaced with more shallow-rooted vegetation. All three modifications reduce infiltration capacities of the soils, which may make classic Horton overland flow a possible runoff mechanism in these areas. The pervious parcels within developed areas may also receive runoff from nearby impervious areas, such as roof drainage onto a lawn, which has a runoff effect analagous to increasing precipitation intensities. Development may also decrease the amount of surface storage available for detaining or retaining runoff, and, because of vegetation changes, can decrease plant interception of rainfall and transpiration of soil moisture.

Using the described possible mechanisms of runoff generation for the study area, seven general hypotheses on the characteristics of rainfall-runoff relations were formulated. With respect to undisturbed, forested areas, four of the general hypotheses apply.

(1) Classical Horton overland flow is not an important runoff mechanism over most, if not all, of these areas.

(2) Subsurface flow, sometimes combined with exfiltration, is the predominant runoff mechanism on hillslopes mantled with glacial till. Within the soil profile, transmission of water is greatly retarded, but once the water is exfiltrated, this mechanism can contribute substantially to storm runoff. The rate of runoff by this mechanism is proportional to the angle of the hillslope.

(3) Ground-water flow is the predominant runoff mechanism on glacial outwash deposits. Runoff rates from this mechanism are slow and attenuated.

(4) Saturation overland flow is the predominant runoff mechanism in depressions, stream bottoms, and till-capped hilltops. Runoff comes quickly and frequently from depressions and stream bottoms, but it comes only during prolonged wet periods from the till-capped hilltops.

With respect to disturbed, nonforested areas, the remaining three of the seven hypotheses apply.

(1) Rapid, direct overland flow is the runoff mechanism on impervious areas.

(2) Horton overland flow, perhaps in combination with some of the mechanisms from undeveloped areas, is an important runoff mechanism from disturbed pervious areas. This is due primarily to changes in soil structure and texture, and to increased moisture supply from nearby impervious surfaces.

(3) There is decreased surface detention and retention storage available, decreased rainfall interception, and decreased plant transpiration in the pervious parcels within disturbed areas.

SIMULATION OF RAINFALL-RUNOFF RELATIONS

The general hypotheses regarding the rainfall-runoff relations are the theoretical foundation of the simulation model. The hypotheses were incorporated into the HSPF framework during model construction, and they were quantified during model calibration.

Construction of the Simulation Model

The study area was divided into 12 types of land segments--1 impervious and 11 pervious--to incorporate the relations into the simulation model. The process-related HSPF parameters were, hence, distributed across the study area in accordance with these land segments. A description of the land segments and their areal extent for the five drainage basins used for model calibration are listed in table 1. The distribution of three of the primary groups of land segments--till, outwash, and saturated--is shown for Big Soos Creek basin in figure 8.

The till segments (TFF, TFM, TFS, TGF, TGM, and TGS) are the areas where a thin, permeable soil covers a nearly impermeable substratum. The first letter in these segment abbreviations (T) reflects that these areas are underlain by basal till or, occasionally, bedrock. The second letter (F or G) reflects the cover condition--F for undisturbed and forested or G for disturbed, with mostly grass vegetation. The third letter (F, M, or S) reflects the slope group--F for 0 to 6 percent, M for 6 to 15 percent, and S for 15 percent and greater.

The TFM and TFS segments represent undisturbed hillslopes where subsurface flow with downslope exfiltration is the predominant runoff mechanism. The TFF segment represents the undisturbed mildly undulating hilltops where saturation overland flow can occur. The TGF, TGM, and TGS segments represent the pervious parcels within disturbed areas where Horton overland flow, as well as the undisturbed area mechanisms, can generate runoff.

The areal extent of the till segments (and all other pervious land segments) was measured directly from maps made from Soil Conservation Service Soil Survey data on soil type and slope, and County agency data on land use and vegetative cover. A list of the Soil Conservation Service soil types found in the study basins (U.S. Department of Agriculture, 1973; 1983) and the land-segment type by which they are represented in the model can be found in table 2.

The outwash soil segments (OF and OG) are the areas, both disturbed and undisturbed, that are mostly covered by soils formed in recessional outwash deposits. Other areas with highly permeable soils and substratum were also included in these segments. The OF segment represents the forested areas where ground-water flow is the predominant runoff mechanism. The disturbed OG segments may also generate Horton overland flow. These two segments were not subdivided into slope groups because slopes in outwash areas are fairly uniform and mild.

Table 1.--Areal extent of land segments found in the five drainage basins used for model calibration

TFF = till soils, forest cover, flat slopes.
TFM = till soils, forest cover, moderate slopes.
TFS = till soils, forest cover, steep slopes.
TGF = till soils, non-forest cover, flat slopes.
TGM = till soils, non-forest cover, moderate slopes.
TGS = till soils, non-forest cover, steep slopes.
OF = outwash soils, forest cover, all slopes.
OG = outwash soils, non-forest cover, all slopes.
CNF = Custer-Norma soils, forest cover, all slopes.
CNG = Custer-Norma soils, non-forest cover, all slopes.
SA = saturated soils, all covers, all slopes.
EIA = effective impervious areas, all slopes.
Cr = creek
abv = above
nr = near
Fk = fork
blw = below
Lk = lake

BASIN NAME	Station	Station location	Land-segment areas (in percent of total area upstream of station)[1]												Total area upstream of station (square
Station name	number	(latitude-longitude)	TFF	TFM	TFS	TGF	TGM	TGS	OF	OG	SA	EIA	CNF	CNG	miles)
QUILCEDA CREEK BASIN															
Quilceda Cr. abv. West Fork nr. Marysville	12157005	48°05'08" 122°10'26"	20.8	4.6	6.3	5.8	0.6	0.6	6.1	11.4	0.2	4.3	4.1	35.1	14.9
West Fk. Quilceda Cr. nr. Marysville	12157020	48°06'07" 122°11'06"	27.4	6.6	6.7	14.2	.6	.5	1.3	.4	.5	3.7	9.7	27.8	9.32
NORTH CREEK BASIN															
Penny Cr. nr. Everett	12125800	47°51'15" 122°12'41"	32.0	.6	2.5	38.5	1.5	.4	0	0	6.3	15.4	0	0	5.53
North Cr. blw. Penny nr. Bothell	12125900	47°49'13" 122°12'42"	31.4	.6	5.9	30.1	.7	.8	1.5	1.9	7.7	18.1	0	0	14.2
North Cr. Tributary nr. Woodinville	12125950	47°49'07" 122°12'24"	38.4	1.3	.9	42.9	1.1	0	0	0	8.1	7.4	0	0	4.51
North Cr. nr. Woodinville	12126100	47°46'48" 122°11'13"	28.7	3.3	6.0	29.9	1.6	.8	4.2	4.6	7.0	13.1	0	0	27.6
SWAMP CREEK BASIN															
Swamp Cr. nr. Alderwood Manor	12126800	47°49'32" 122°15'15"	31.4	6.5	4.1	22.9	4.3	1.4	1.7	.9	6.4	20.1	0	0	8.90
Scriber Cr. nr. Mountlake Terrace	12126900	47°47'58" 122°15'27"	14.0	4.4	4.3	37.3	4.1	.2	0	0	3.2	32.4	0	0	6.98
Swamp Cr. nr. Kenmore	12127100	47°45'22" 122°13'57"	21.2	6.1	5.6	26.6	5.4	1.0	4.2	3.3	5.8	20.6	0	0	23.6

Table 1.--Areal extent of land segments found in the five drainage basins used for model calibration--continued

BASIN NAME Station name	Station number	Station location (latitude-longitude)	Land segment areas (in percent of total area upstream of station)[1]												Total area upstream of station (square miles)
			TFF	TFM	TFS	TGF	TGM	TGS	OF	OG	SA	EIA	CNF	CNG	
BEAR CREEK BASIN															
Bear Cr. nr. Redmond	12122500	47°45'25" 122°09'50"	13.1	62.5	4.3	.7	3.9	0	4.6	1.7	7.6	1.0	0	0	14.2
Cottage Lk. Cr. abv. Bear nr. Redmond	12123100	47°43'03" 122°05'07"	17.2	41.4	2.5	5.3	8.5	.1	8.6	4.3	7.3	3.4	0	0	12.6
Bear Cr. Tributary nr. Redmond	12123200	47°42'02" 122°04'08"	-	68.9	8.0	.5	10.6	0	10.8	0	.6	.7	0	0	1.28
Evans Cr. abv. Mouth nr. Redmond	12124000	47°40'32" 122°04'48"	2.3	38.8	9.0	2.0	10.8	.4	15.3	6.4	11.2	3.7	0	0	14.6
Bear Cr. at Redmond	12124500	47°40'29" 122°06'25"	8.7	46.5	5.0	2.2	9.2	.3	10.8	5.3	8.6	3.0	0	0	50.7
BIG SOOS CREEK BASIN															
Little Soos Cr. nr. Kent	12109500	47°22'22" 122°06'46"	1.1	69.8	0.7	3.1	9.6	0	7.5	1.9	4.8	2.8	0	0	2.85
Big Soos Cr. abv. Jenkins nr. Auburn	12110000	47°20'38" 122°08'00"	13.6	27.5	3.7	10.9	14.0	1.0	9.3	1.9	9.9	7.0	0	0	18.6
South Fork Jenkins Cr. nr. Covington	12110400	47°21'22" 122°05'02"	2.9	8.6	0	.3	4.8	0	64.4	7.8	7.0	4.3	0	0	3.51
Jenkins Cr. nr. Auburn	12110500	47°20'24" 122°07'42"	3.9	22.5	1.9	1.1	6.1	.1	40.0	12.5	5.6	4.6	0	0	16.0
Covington Cr. nr. Auburn	12112000	47°18'51" 122°06'32"	0	36.4	7.1	0	4.1	.6	37.2	3.9	5.6	1.7	0	0	20.6
Soosette Cr. nr. Auburn	12112550	47°19'03" 122°09'30"	20.0	23.2	8.1	15.2	15.1	1.4	3.8	1.3	5.8	5.9	0	0	5.44
Big Soos Cr. abv. Hatchery nr. Auburn	12112600	47°18'35" 122°10'05"	7.1	27.2	5.6	4.7	8.1	.6	28.1	5.4	6.8	4.5	0	0	65.8

[1] When the sum of the percentages is less than 100, the remaining area is covered by open water.

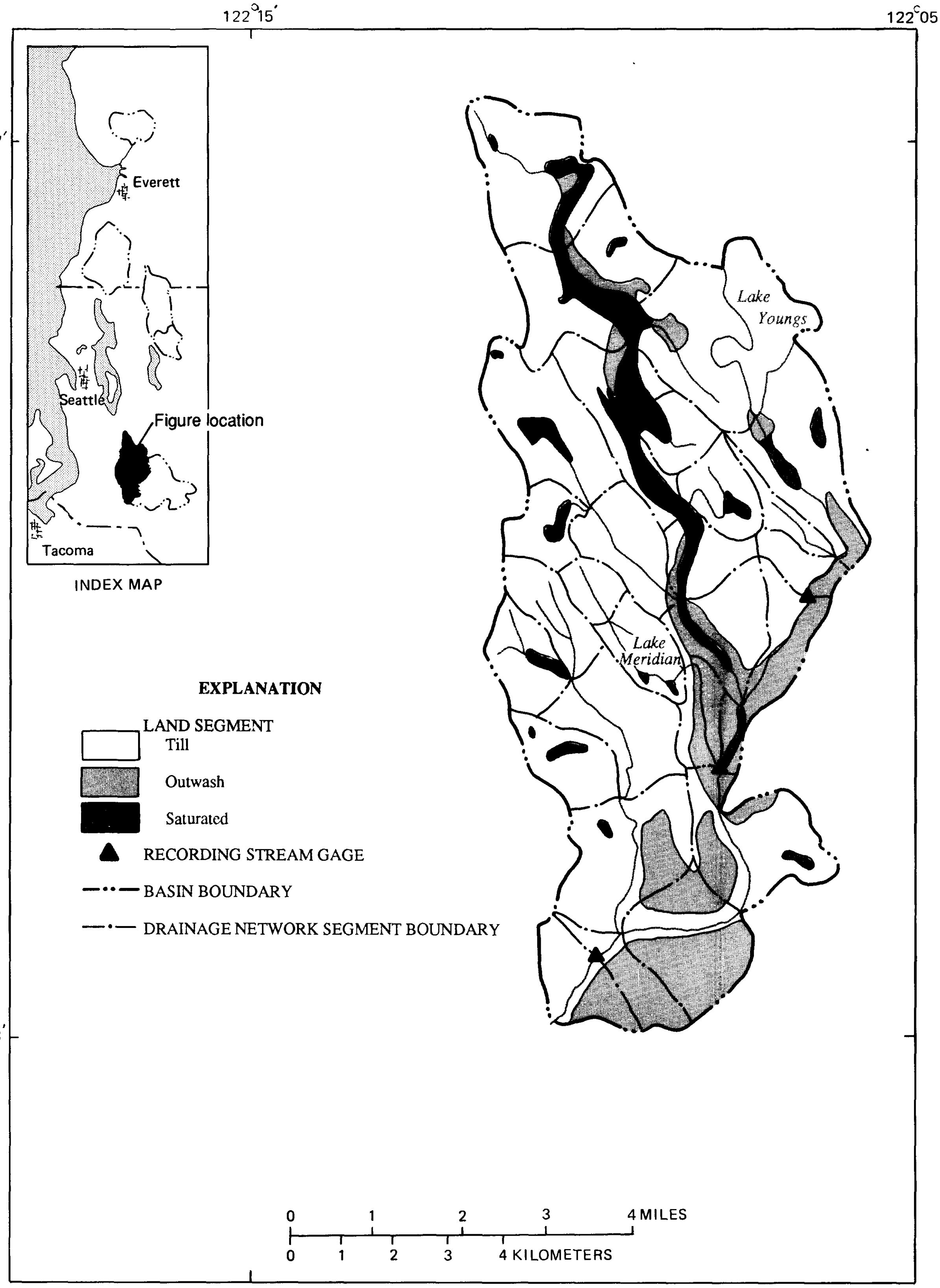

Figure 8.--Distribution of till, outwash, and saturated land segments, and drainage network segmentation in Big Soos Creek basin.

Table 2.--Soil series found in the calibration basins and the land-segment soil type they were represented by in the model (U. S. Department of Agriculture, 1973, 1983)

Land-segment soil type	King County soil type	Snohomish County soil type
Till	Alderwood gravelly sandy loam	Alderwood gravelly sandy loam
	Arents, Alderwood material	Alderwood-Everett gravelly sandy loam
	Beausite gravelly sandy loam	Alderwood-Urban land complex
	Kitsap silt loam	Kitsap silt loam
		McKenna gravelly silt loam
		Pastik silt loam
		Tokul silt loam
		Tokul gravelly loam
		Tokul-Winston gravelly loams
Outwash	Arents, Everett material	Everett gravelly sandy loam
	Everett gravelly sandy loam	Indianola loamy sand
	Indianola loamy fine sand	Lynnwood loamy sand
	Mixed alluvial land	Ragnar fine sandy loam
	Neilton very gravelly loamy sand	
	Puyallup fine sandy loam	
	Ragnar fine sandy loam	
	Ragnar-Indianola association	
Saturated	Bellingham silt loam	Bellingham silty clay loam
	Briscot silt loam	Mukilteo muck
	Norma sandy loam	Norma loam
	Orcas peat	Norma variant loam
	Renton silt loam	Orcas peat
	Seattle muck	Puget silty clay loam
	Shalcar muck	Sumas silt loam
	Snohomish silt loam	Terric medisaprists
	Sultan silt loam	
	Tukwila muck	
Custer-Norma[1]		Custer fine sandy loam
		Norma loam
		Norma variat loam
Effective impervious area	Urban land	Urban land

[1]Norma soils were included in the Custer-Norma segments when they were present in the Marysville trough area of Quilceda Creek basin, and were included in the Saturated segment in all other areas.

The Custer-Norma segments (CNF and CNG) are additional areas, both forested and nonforested, where high water tables can generate saturated overland flow. These segments, however, are underlain by substratum more permeable than basal till, and are all nearly flat-lying. They are exclusive to the Marysville area north of the city of Everett.

The saturated segments (SA) are the bottomland or depressional areas with a seasonally high water table that can generate substantial amounts of saturated overland flow. These segments generally include only those areas that are seasonally inundated; perennial wetlands, along with ponds and lakes, are included as part of the drainage network of a basin.

The land segments labeled effective impervious area (EIA) are those areas with direct runoff from impervious surfaces. The segments are composed only of impervious surfaces where surface runoff is directly connected to the drainage network. The extent of EIA in a basin was determined by first measuring the areas covered by five land-use types: low-density development (one unit per 2 to 5 acres); medium-density development (one unit per acre); suburban development (four units per acre); high-density development (multi-family or high-density housing); and commercial, industrial, and transportation facilities. The amount of area within these five land-use types that is actually covered with impervious surfaces was estimated to be 10 percent, 20 percent, 35 percent, 60 percent, and 90 percent of the total area measured for each respective land-use type (Alley and Veenhuis, 1983; Laenen, 1983; Prych, 1986). The amount of EIA within the five land-use types was then estimated to be 40 percent, 50 percent, 66 percent, 80 percent, and 95 percent of the total impervious area of each land-use type, respectively (Alley and Veenhuis, 1983). These percentage estimates are based on the assumption that not all impervious surfaces, particularly rooftops, are directly connected to the drainage network.

The estimates were used for determining EIA in all areas except for the Scriber Creek basin, a tributary to Swamp Creek. An extensive pipe storm-drain system connects almost all impervious surfaces to the drainage network in the Scriber Creek area, so all of the impervious area was considered to be effective. In all other basins, the impervious areas considered to be noneffective were included in the adjacent pervious land segments onto which they drain. The noneffective impervious area in low-density development areas was divided between forested and nonforested segments, whereas the noneffective impervious area in the other land-use types was all assumed to be nonforested.

Another phase of model construction required division of the drainage network of a basin into segments called reaches, each with relatively uniform hydraulic properties. Segmentation of the Big Soos Creek drainage network is shown in figure 8. It is here where the hydraulic characteristics of the drainage system, including lakes and wetlands, were represented in the simulation model. Because the model parameters representing these hydraulic properties can be computed directly from field measurements, it was not necessary to generalize channel characteristics. As with basin segmentation, channel segmentation was somewhat generalized to simulate only the essential hydraulic characteristics of a drainage network, rather than to simulate the flow through every pipe, ditch, pond, and channel found in the study basins.

The drainage networks in the study basins were divided into a total of 170 reaches, each with its own subbasin drainage area. A volume-discharge relation was determined for each reach by first identifying and characterizing the primary hydraulic control within the reach (generally located at the downstream end of the reach), and then estimating the amount of surface-water storage available in the reach for a number of known discharge values at the control. The hydraulic characteristics of the control points were determined by field measurements for the data needed to apply Manning's equation for open channels and the energy equation for culverts, pipes, or contracted openings. The storage volumes corresponding to discharge rates at the control were estimated by field and map measurements of channel, pipe, lake, and wetland geometries.

The runoff from the various segments within each subbasin was assigned to drain into the appropriate channel reach using the NETWORK block of the HSPF model. Some important ground-water-related features that are not represented by process-related model parameters in the HSPF model were incorporated into this NETWORK block.

The first feature incorporated into the NETWORK block involved ground-water recharge and discharge areas. Ground water that is recharged in the delineated subbasins of the region does not always discharge to streams within the same subbasin. Some general guidelines were followed to delineate ground-water recharge areas and to identify which subbasins are areas of discharge.

The first guideline was that all ground-water recharge in outwash, Custer-Norma, and valley-bottom saturated segments was assumed to discharge within the same subbasin. These segments are most commonly found in or near the stream valleys where ground-water tables are near the ground surface.

The second guideline was that ground-water recharge in upland till or saturated segments was assumed to discharge at the first downgradient location where till is no longer mantling the surface. This location was not always within the same subbasin where recharge was occurring. For example, if a subbasin composed entirely of till segments was located upgradient from a subbasin with outwash segments, the recharge from both subbasins was assumed to discharge in the outwash-covered subbasin only. The assumption behind this guideline is that flow through the till is vertical and flow through the more permeable layers below the till is horizontal.

If reported information about ground-water flow suggested that recharge water from any segment did not discharge anywhere in the drainage basin, then that recharge water was not allowed to discharge in the simulation model either. Some general geologic and ground-water information from three available published reports (Liesch and others, 1963; Luzier, 1969; Newcomb, 1952) was used to help delineate recharge and discharge areas.

The second feature incorporated into the NETWORK block involved subsurface-flow discharge areas. It was generally assumed that this runoff from the till hillslopes would discharge in the same subbasin in which it was recharged. An exception to this was made in the Jenkins Creek and Covington Creek basins. The physiography of these basins is somewhat unique in that exceptionally deep and widespread glacial outwash deposits cover most of the area of these basins. The till that is the predominant surface material in most other basins in the study region is exposed only at the surface in small upland parcels in the Jenkins Creek and Covington Creek basins. It was estimated from soils and topographic maps that about 50 percent of the till area in Jenkins Creek basin generates subsurface flow that, even after exfiltration, would flow into downslope outwash deposits, rather than into a channel reach. About 80 percent of the till area in Covington Creek basin was estimated to do likewise. Hence, the appropriate volumes of subsurface flow from these till segments were routed into the ground-water system of downslope outwash segments in the NETWORK block of the simulation model.

Calibration of the Simulation Model

The initial estimates of the process-related parameters were set so that each land segment would generate runoff relative to other land segments in accordance with the hypothesized mechanisms of each. For example, parameters for saturated areas were set to give a rapid hydrologic response, parameters for outwash areas were set to give a greatly delayed response, and parameters for till areas fell in between. Throughout the trial-and-error procedure to adjust parameters, these relative hydrologic responses between the land segments were held constant. The parameters were adjusted to quantify the rate and magnitude of the responses; the hypothesized qualitative nature of the responses was assumed to be correct.

The model parameters derived by calibration for the 12 land-segment types are given in table 3. The following is a brief description of how these parameters relate to the runoff mechanisms hypothesized for each segment.

Simulated runoff from undisturbed till-mantled hillslope segments (TFM and TFS) was controlled primarily by the low INFILT values and high INTFW values. The INFILT values were low enough to restrict vertical drainage from the soil mantle, but they were high enough, in combination with high INTFW values, to allow for a large subsurface flow component of runoff near the ground surface. The steep slope segment had better drainage (a lower INFEXP) and a quicker subsurface flow response (lower IRC) than the moderate slope segment.

Simulated runoff from disturbed till-mantled hillslope segments (TGM and TGS) was controlled primarily by the low INFILT values. Some overland flow was generated from these segments during large storms, as well as some subsurface flow. Runoff retention and detention, represented by UZSN, and evapotranspiration, represented by LZETP, were less in these segments than in the comparable undisturbed segments.

Simulated runoff from the flat-slope till segments (TFF and TGF) was similar to, but slower than, that from their steeper sloped counterparts during small storms. However, the high INFEXP allowed both of these flat segments to generate substantial quantities of overland flow during large storms.

Table 3.--Generalized model parameters representing the 12 calibrated land segments

[Units are printed below parameter name; where units are not listed, the parameter has no units. Land-segment definitions: TFF = till soils, forest cover, flat slopes; TFM = till soils, forest cover, moderate slopes; TFS = till soils, forest cover, steep slopes; TGF = till soils, non-forest cover, flat slopes; TGM = till soils, non-forest cover, moderate slopes; TGS = till soils, non-forest cover, steep slopes; OF = outwash soils, forest cover, all slopes; OG = outwash soils, non-forest cover, all slopes; CNF = Custer-Norma soils, forest cover, all slopes; CNG = Custer-Norma soils, non-forest cover, all slopes; SA = saturated soils, all covers, all slopes; EIA = effective impervious areas, all slopes. LZSN = lower-zone nominal storage; INFILT = infiltration capacity; LSUR = average length of the overland flow plane; SLSUR = average slope of the overland flow plane; KVARY = ground-water outflow modifier; AGWRC = ground-water recession parameter; INFEXP = infiltration equation exponent; INFILD = ratio of the maximum to mean infiltration rate of a pervious area; BASETP = fraction of available-PET demand that can be met with ground-water outflow; AGWETP = fraction of available-PET demand that can be met with stored ground water; CEPSC = interception storage capacity of plants; UZSN = upper-zone nominal storage; NSUR = average roughness of the overland flow plane; INTFW = interflow index; IRC = interflow recession parameter; LZETP = lower-zone ET; RETSC = retention storage capacity of impervious areas; in. = inches; in./hr = inches per hour; ft = feet; 1/in. = 1/inch; n/a = not applicable.]

	Model Parameter																
Land Segment	LZSN (in.)	INFILT (in./hr)	LSUR (ft.)	SLSUR	KVARY (1/in.)	AGWRC (1/day)	INFEXP	INFILD	BASETP	AGWETP	CEPSC (in.)	UZSN (in.)	NSUR	INTFW	IRC (1/day)	LZETP	RETSC (in.)
TFF	4.5	0.08	400	0.05	0.5	0.996	3.5	2.0	0.0	0.0	0.2	1.0	0.35	3.0	0.7	0.7	n/a
TFM	4.5	.08	400	.10	.5	.996	2.0	2.0	.0	.0	.2	.5	.35	6.0	.5	.7	n/a
TFS	4.5	.08	200	.20	.5	.996	1.5	2.0	.0	.0	.2	.3	.35	7.0	.3	.7	n/a
TGF	4.5	.03	400	.05	.5	.996	3.5	2.0	.0	.0	.1	.5	.25	3.0	.7	.25	n/a
TGM	4.5	.03	400	.10	.5	.996	2.0	2.0	.0	.0	.1	.25	.25	6.0	.5	.25	n/a
TGS	4.5	.03	200	.20	.5	.996	1.5	2.0	.0	.0	.1	.15	.25	7.0	.3	.25	n/a
OF	5.0	2.00	400	.05	.3	.996	2.0	2.0	.0	.0	.2	.5	.35	.0	.7	.7	n/a
OG	5.0	.80	400	.05	.3	.996	2.0	2.0	.0	.0	.1	.5	.25	.0	.7	.25	n/a
CNF	2.0	.40	400	.01	4.0	.990	3.5	2.0	.0	.0	.2	1.0	.35	4.0	.8	.9	n/a
CNG	2.0	.16	400	.01	4.0	.990	3.5	2.0	.0	.0	.1	.5	.25	4.0	.8	.9	n/a
SA	4.0	2.00	100	.001	.5	.996	10.0	2.0	.0	.7	.1	3.0	.50	1.0	.7	.8	n/a
EIA	n/a	n/a	500	.01	n/a	n/a	n/a	n/a	n/a	n/a	n/a	n/a	.10	n/a	n/a	n/a	.10

Simulated runoff from both outwash segments (OF and OG) was controlled primarily by high INFILT values and low INTFW values. These parameters allowed a nearly exclusive ground-water-flow response from these segments, with some overland flow possible from the disturbed segment during intense storms.

Simulated runoff from the Custer-Norma segments (CNF and CNG) was controlled primarily by moderate INFILT values, moderate INTFW values, and high INFEXP values. These resulted in a slow subsurface flow response during small storms, and an overland flow response during larger storms. As with the other segments, the overland flow was more substantial from the disturbed segment.

Finally, simulated runoff from the saturated segment (SA) was controlled by a large INFILT, a large INFEXP, and a large UZSN. This resulted in no runoff during small storms in the dry season, and nearly 100 percent overland flow during the largest wet-season storms. The impervious segment (EIA) generated overland flow only.

The following information is indicative of simulation-model performance for the period of calibration. Observed and simulated values of annual and seasonal runoff and the difference between simulated and observed values, in units of inches and percent, are shown in table 4. Runoff, as used in this table, is the total volume of streamflow recorded at the gage sites for the stated period. Observed and simulated runoff volumes and peak discharge rates for selected storms and the difference between simulated and observed values in units of inches and percent, are shown in table 5. These volumes and discharges represent the four highest streamflow periods for which complete records of observed rainfall and streamflow data were available for each gaged basin. Comparisons of the observed and simulated annual, seasonal, storm peak discharge, and storm runoff values are also shown in figure 9, and six typical observed and simulated storm hydrographs are shown in figures 10 through 15. All of the daily mean discharges used for calibration are not shown for all of the stream-gaging stations included in this report, but typical daily flow hydrographs that were observed and simulated for the 2-year calibration period are shown for six of the stations in figures 16 through 21. Statistical measures of the errors in simulating daily mean flows at each gaging station are given in table 6.

The composite simulation errors for all of the streamflow gages and basins in the region, as evaluated by several methods, are summarized in table 7. The mean absolute error is the average of differences between simulated and observed runoff, disregarding whether the difference was positive or negative. The root mean square error is the standard deviation of the differences. Two-thirds of all the errors should be less than or equal to this value. The bias is the average of differences between simulated and observed runoff with regard to the sign of individual differences. A large positive bias means that the model is, in general, overestimating streamflow, and a large negative bias means that it is underestimating streamflows. The standard error of estimate is the standard deviation of the differences after accounting for the bias. Standard error of estimate is nearly equal to root mean square error for data with little bias.

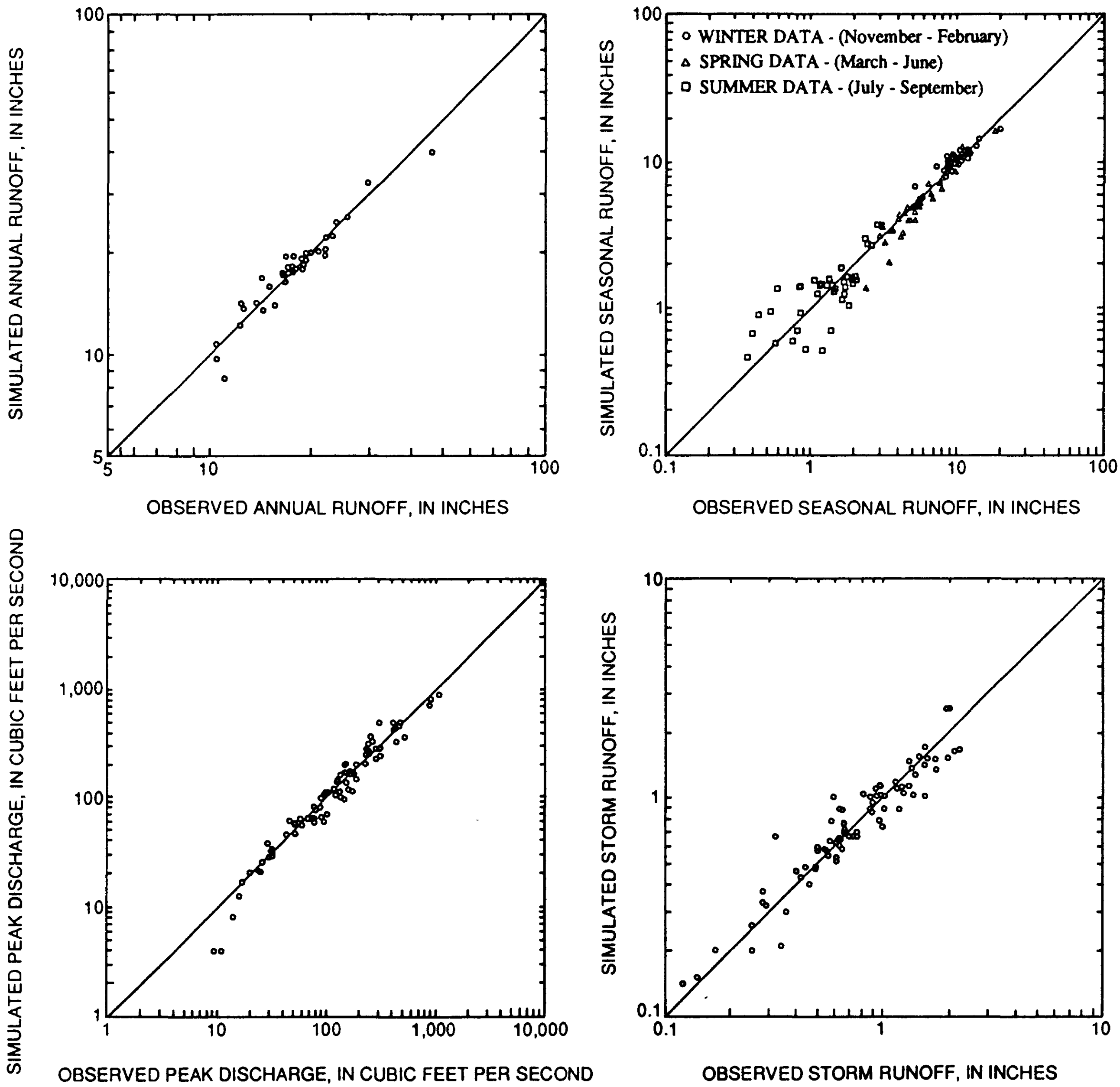

Figure 9.--Observed and simulated annual runoff, seasonal runoff, storm runoff, and peak discharge data used for model calibration.

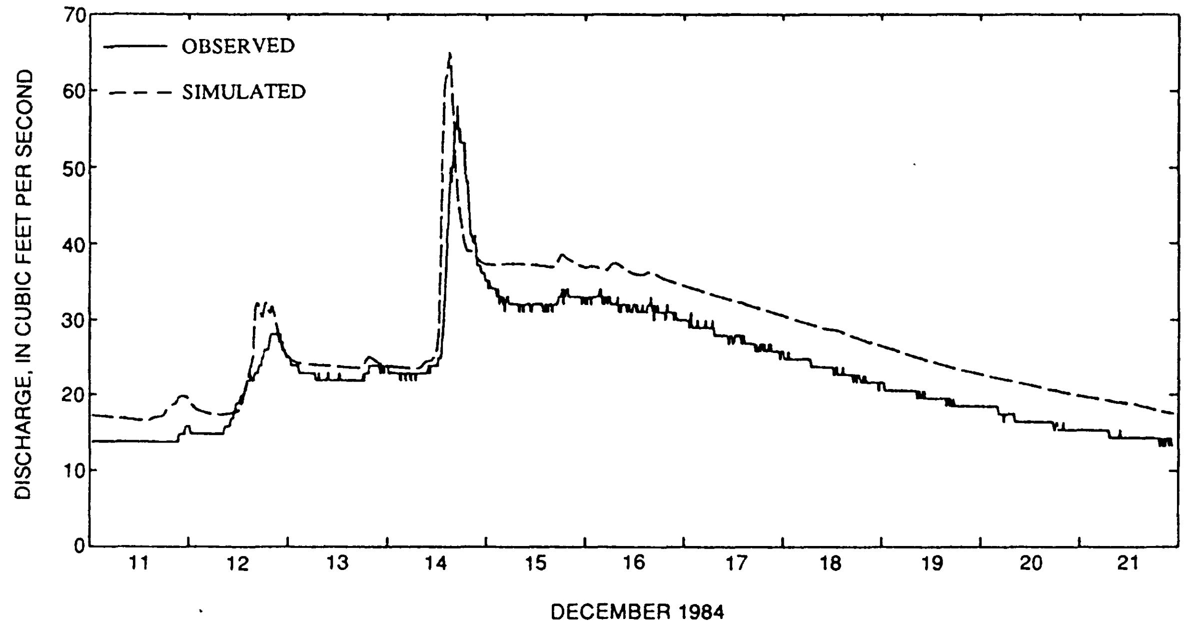

Figure 10.--Observed and simulated discharge for Penny Creek (Station 12125800) in the North Creek basin, storm period December 11-21, 1984.

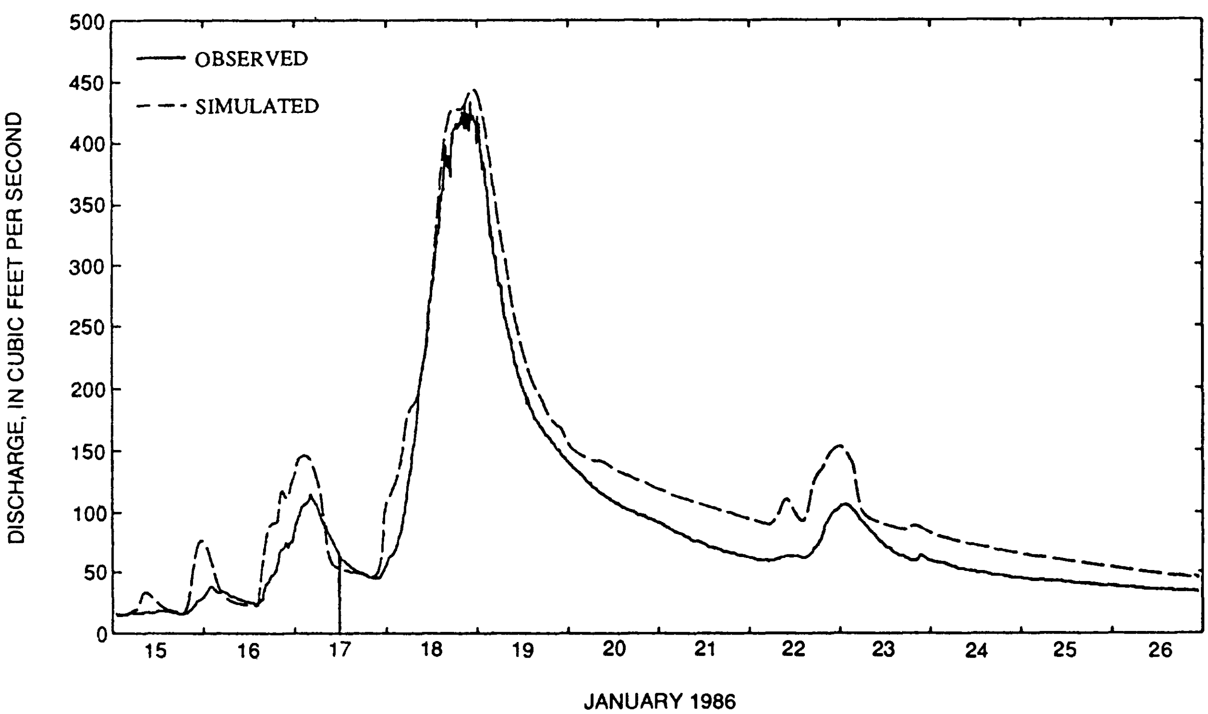

Figure 11.--Observed and simulated discharge for Upper North Creek (Station 12125900) in the North Creek basin, storm period January 15-26, 1986.

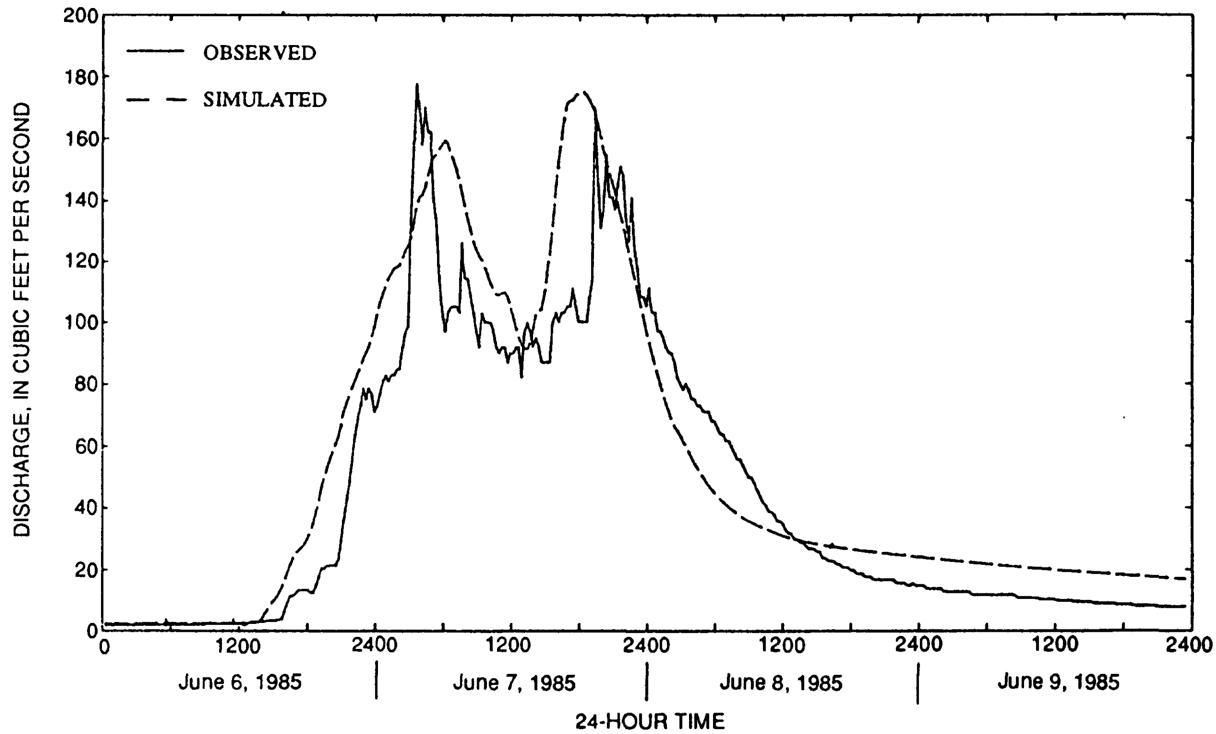

Figure 12.--Observed and simulated discharge for Scriber Creek (Station 12126900) in the Swamp Creek basin, storm period June 6-9, 1985.

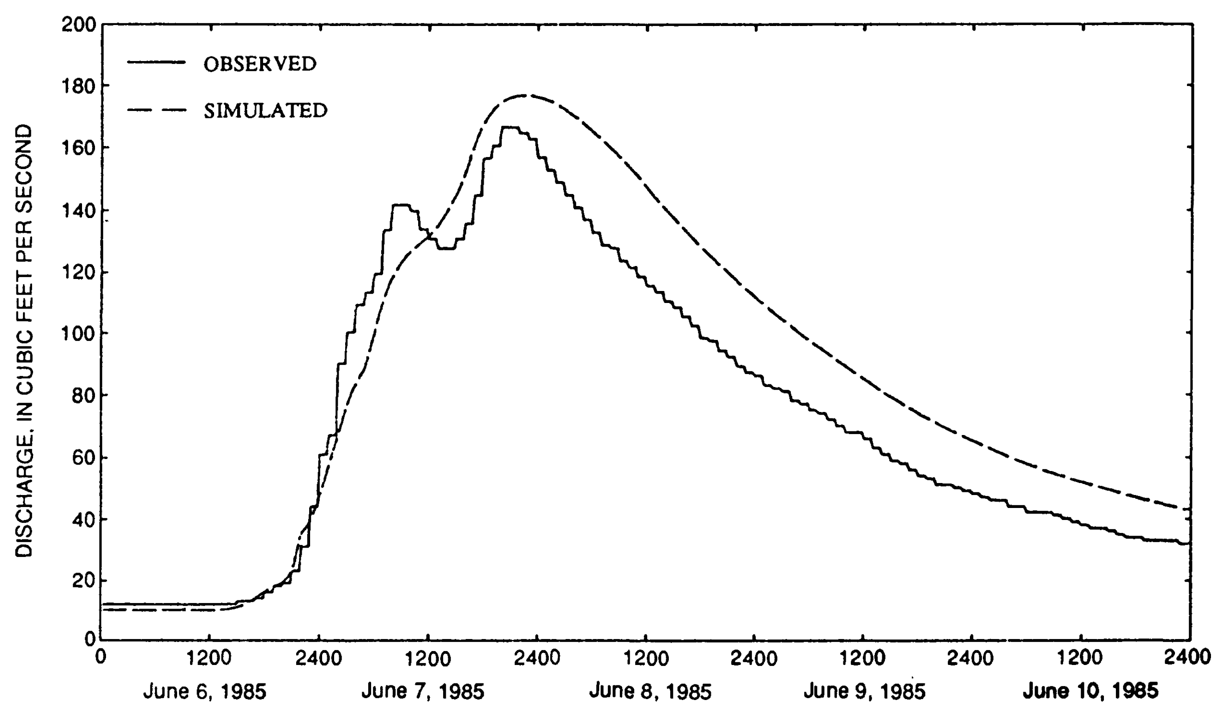

Figure 13.--Observed and simulated discharge for Upper Bear Creek (Station 12122500) in the Bear and Evans Creek basins, storm period June 6-10, 1985.

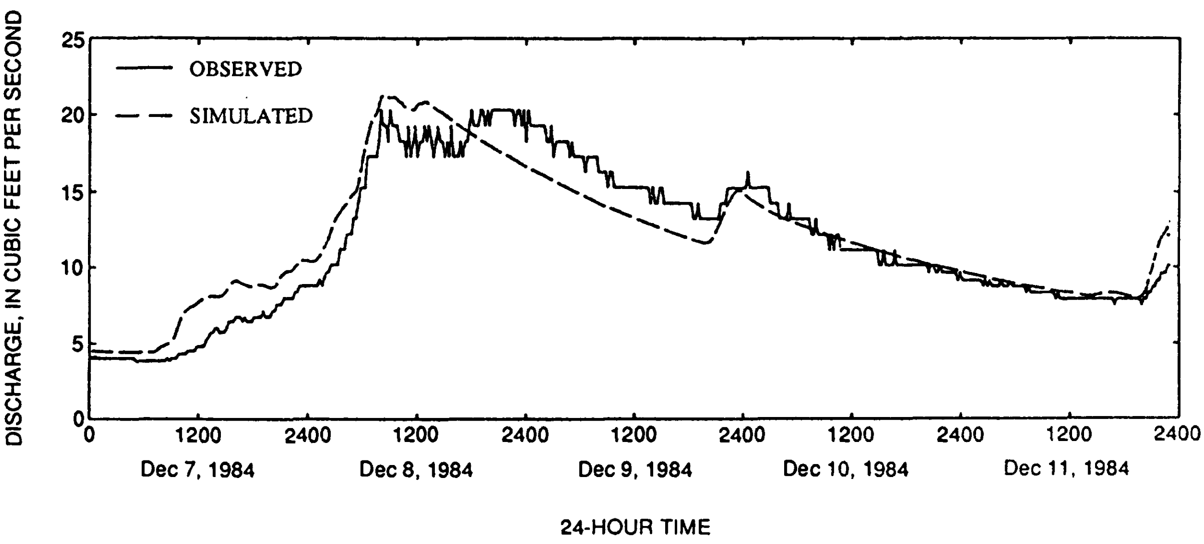

Figure 14.--Observed and simulated discharge for Little Soos Creek (Station 12109500) in the Big Soos Creek basin, storm period December 7-11, 1984.

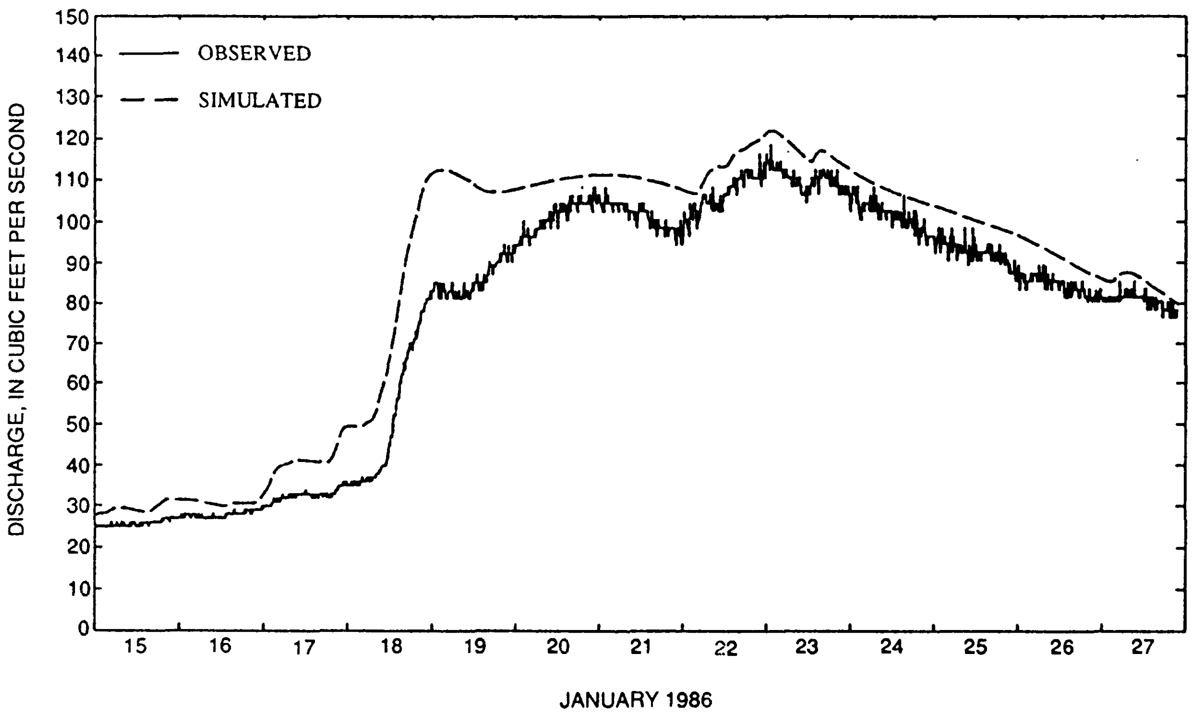

Figure 15.--Observed and simulated discharge for Covington Creek (Station 12112000) in the Bog Soos Creek basin, storm period January 15-27, 1986.

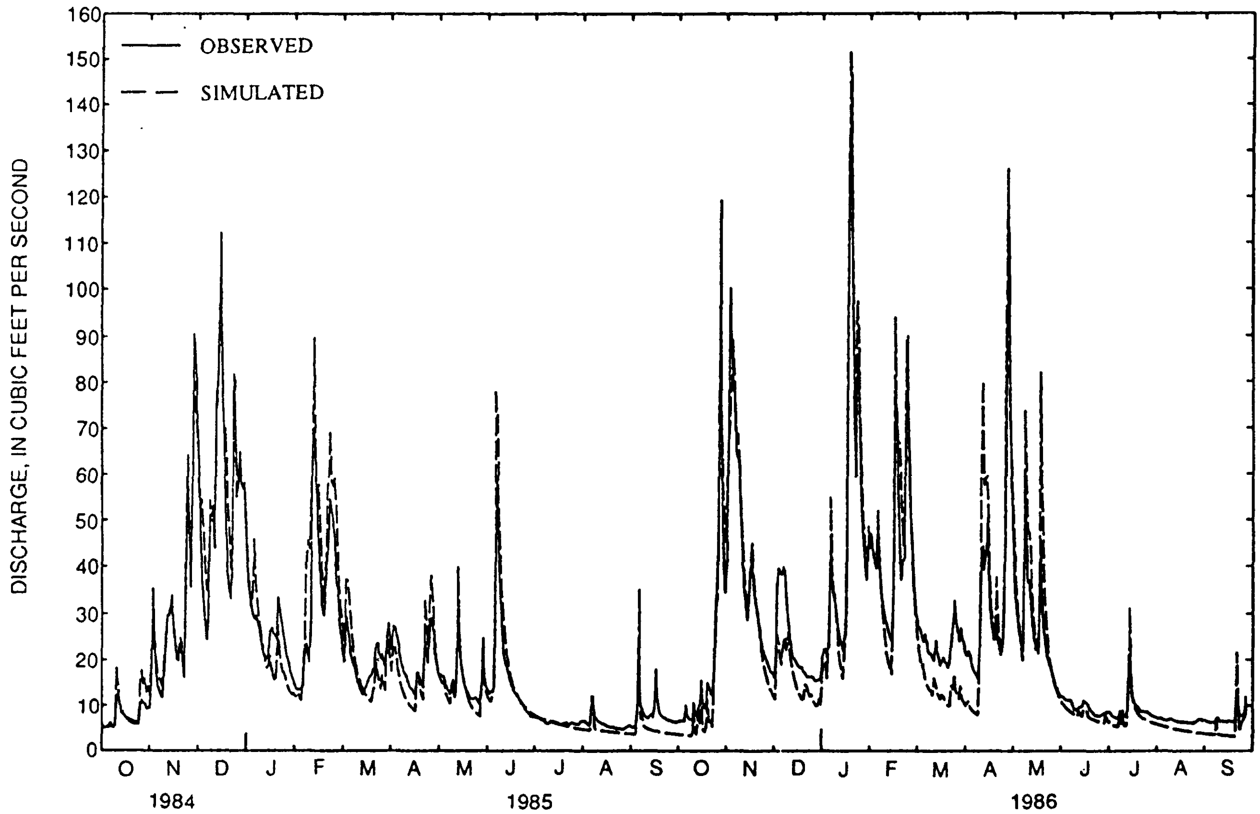

Figure 16.--Observed and simulated daily mean discharge for Quilceda Creek (station 12157005) in the Quilceda Creek basin, October 1984 - September 1986.

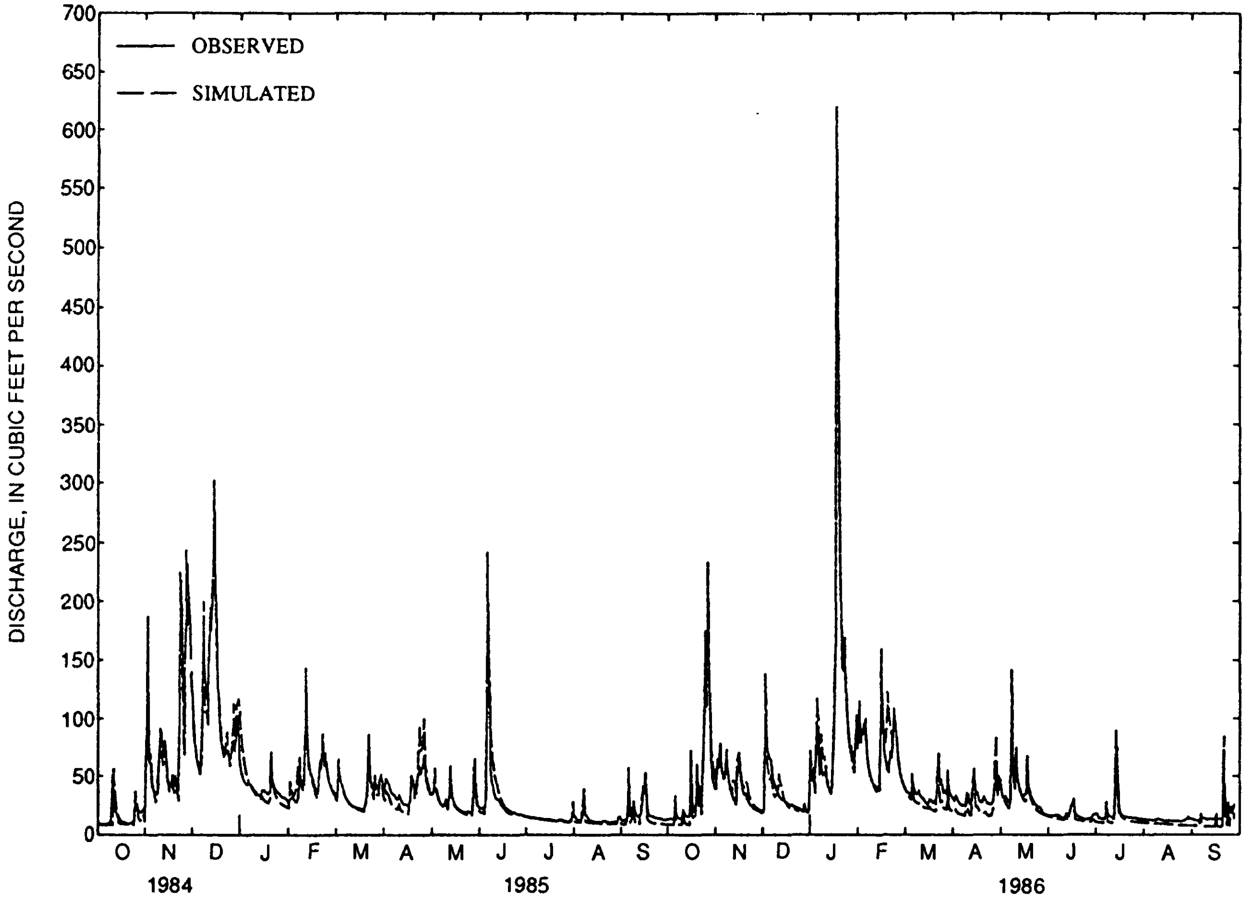

Figure 17.--Observed and simulated simulated daily mean discharge for North Creek (station 12126100) in the North Creek basin, October 1984 - September 1986.

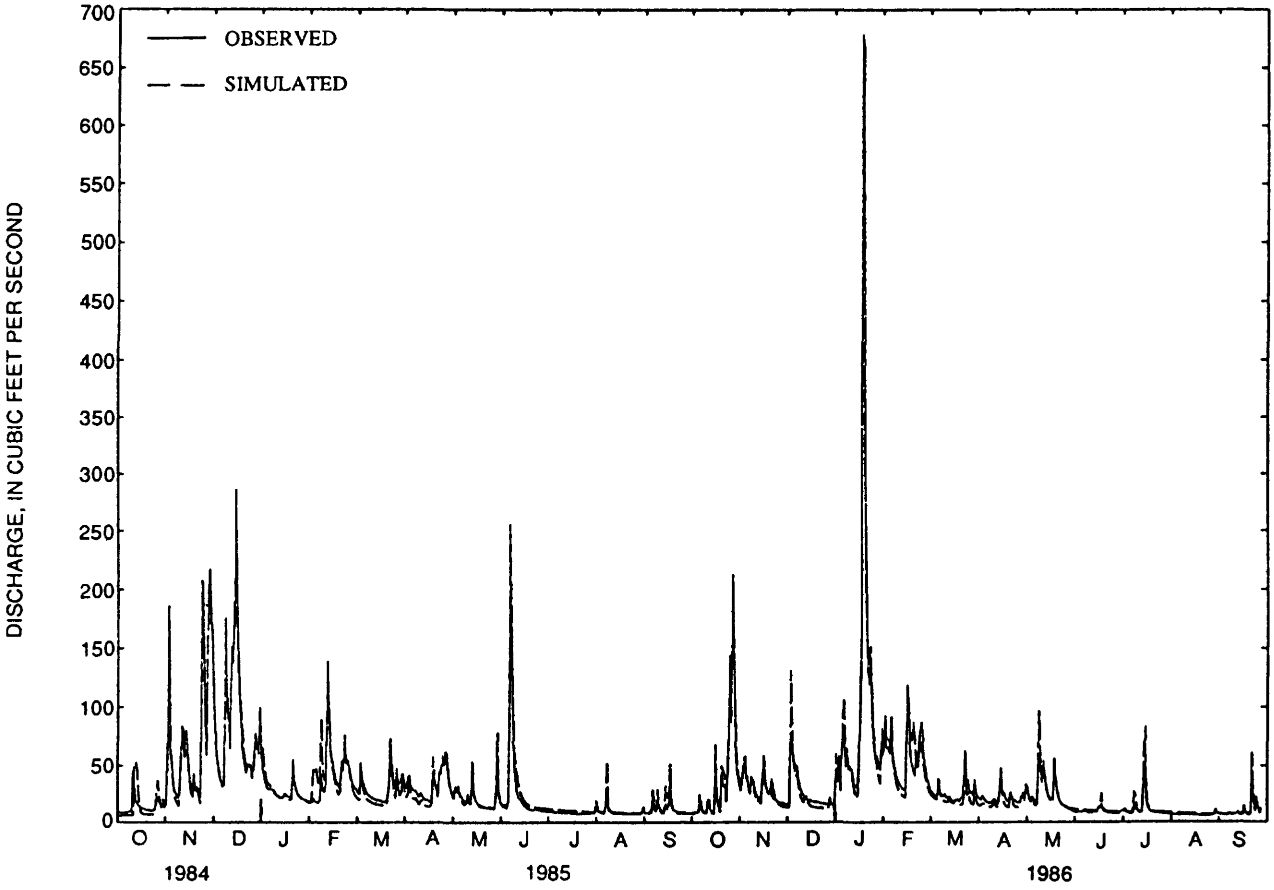

Figure 18.--Observed and simulated daily mean discharge for Swamp Creek (station 12127100) in the Swamp Creek basin, October 1984 - September 1986.

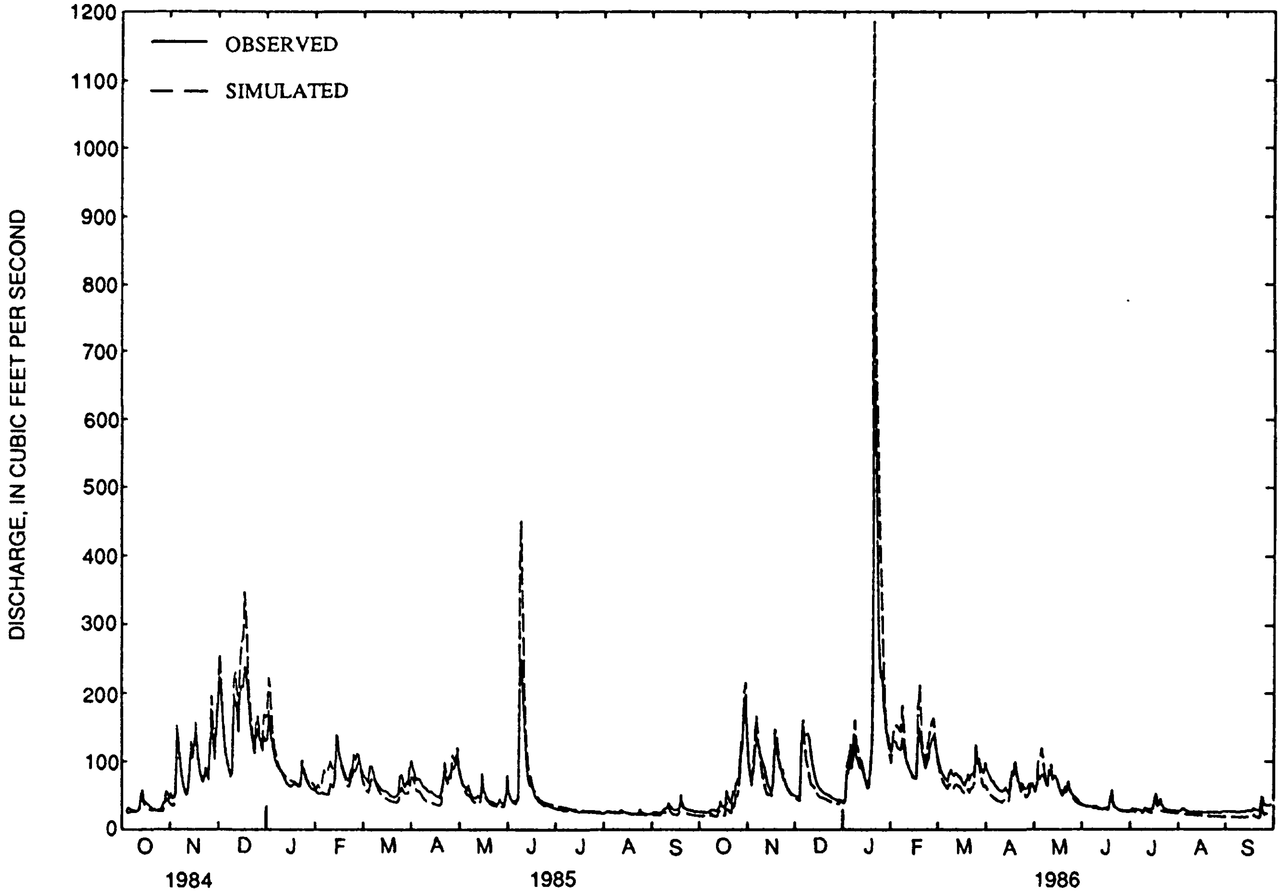

Figure 19.--Observed and simulated daily mean discharge for Bear Creek (station 12124500) in the Bear and Evans Creek basins, October 1984 - September 1986.

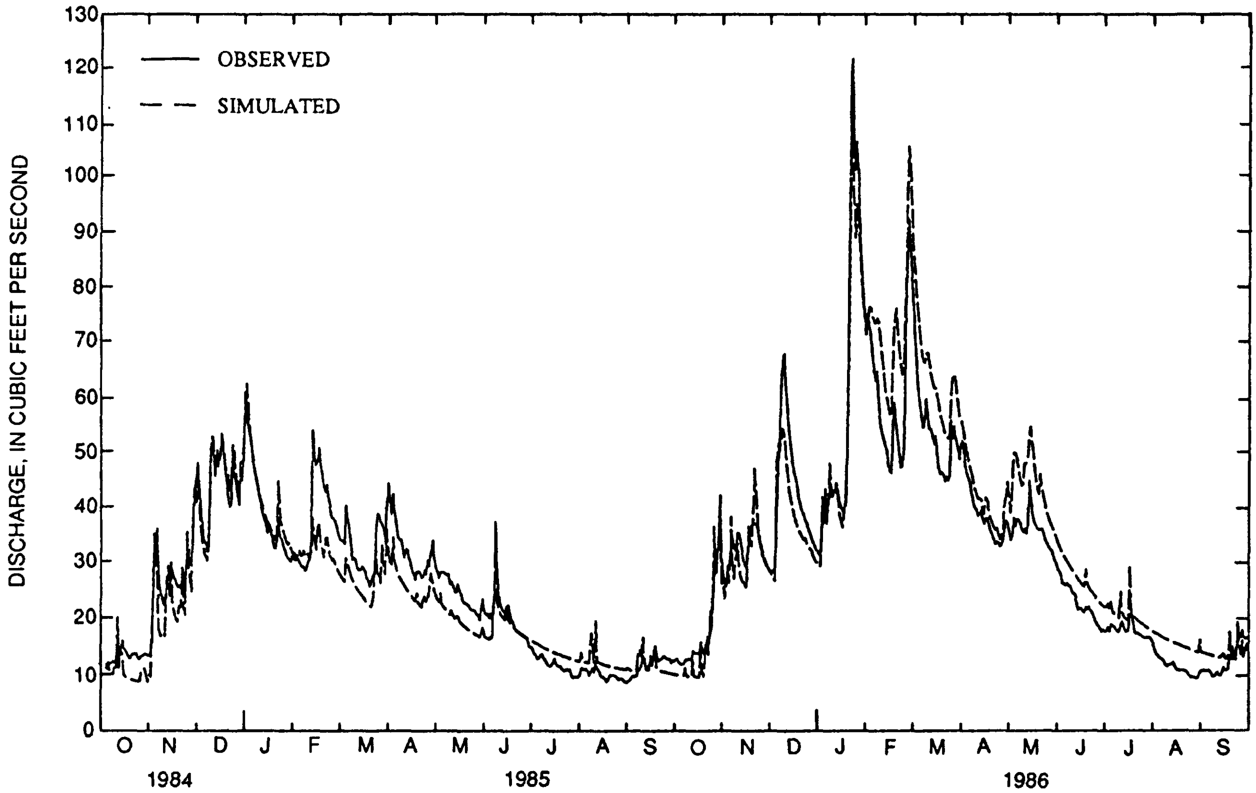

Figure 20.--Observed and simulated daily mean discharge for Jenkins Creek (station 12110500) in the Big Soos Creek basin, October 1984 - September 1986.

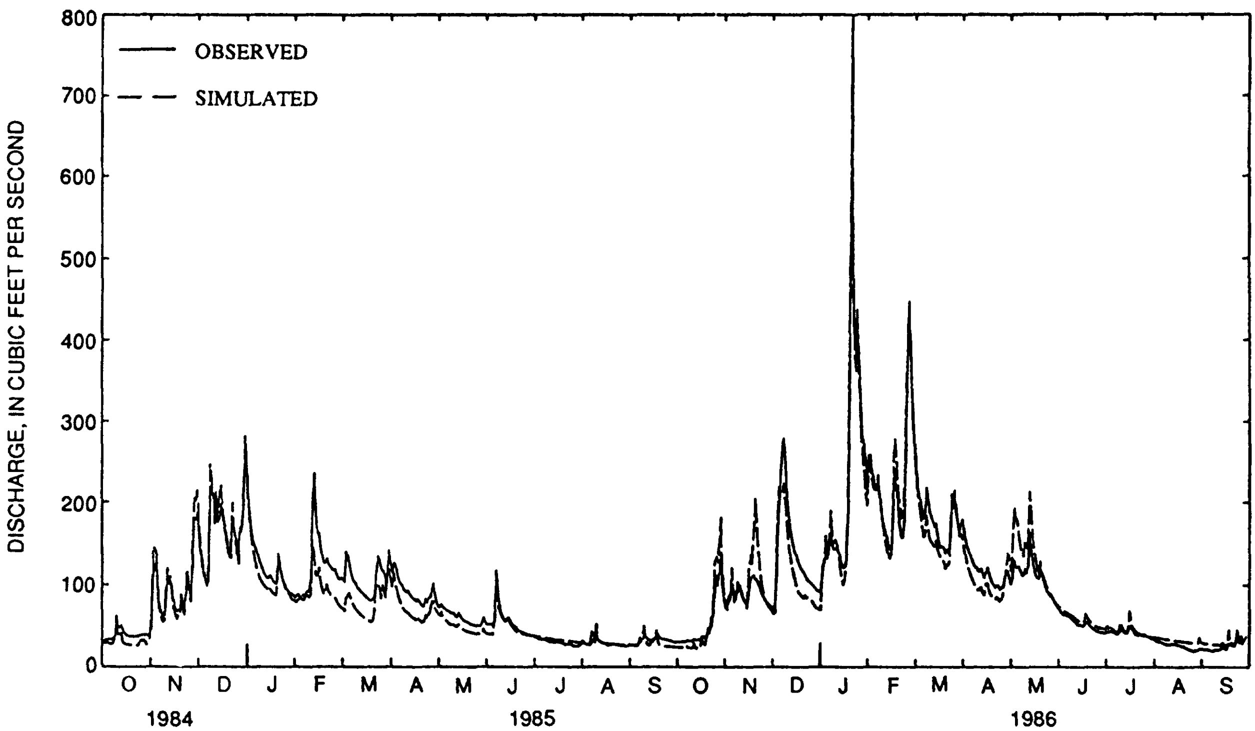

Figure 21.--Observed and simulated daily mean discharge for Big Soos Creek (station 12112600) in the Big Soos Creek basin, October 1984 - September 1986.

Table 4.--Observed and simulated annual and seasonal runoff data

[Obs. = Observed value, in inches; Sim. = Simulated value, in inches; Difference, inches = Sim. - Obs., in inches; Difference, percent = 100 x [(Sim. - Obs.)/Obs.], in percent.]

		Annual runoff[1]				Winter runoff[2]				Spring runoff[3]				Summer runoff[4]			
				Difference				Difference				Difference				Difference	
Station number	Water year	Obs.	Sim.	Inches	Percent	Obs.	Sim.	Inches	Percent	Obs.	Sim.	Inches	Percent	Obs.	Sim.	Inches	Percent
12157005	1985	19.24	19.85	0.61	3.2	11.24	11.98	0.74	6.6	5.65	5.73	0.08	1.4	1.72	1.38	-0.34	-19.8
	1986	23.18	22.27	-.91	-3.9	11.97	11.81	-.16	-1.3	7.62	7.44	-.18	-2.4	2.02	1.64	-.38	-18.8
12157020	1985	14.20	16.79	2.59	18.2	8.48	11.00	2.52	29.7	4.37	4.49	.12	2.8	.80	.70	-.10	-12.5
	1986	18.65	19.13	.48	2.6	10.09	10.74	.65	6.4	6.66	6.11	-.55	-8.3	.84	.93	.09	10.7
12125800	1985	13.68	14.14	.46	3.4	8.51	9.23	.72	8.5	3.98	4.10	.12	3.0	.74	.59	-.15	-20.3
	1986	12.34	14.10	1.76	14.3	7.18	9.34	2.16	30.1	3.60	3.39	-.21	-5.8	.91	.52	-.39	-42.9
12125900	1985	19.98	19.95	-.03	-.2	11.39	11.89	.50	4.4	5.85	5.89	.04	.7	1.91	1.60	-.31	-16.2
	1986	17.68	19.43	1.75	9.9	9.35	11.34	1.99	21.3	4.83	4.91	.08	1.7	2.06	1.55	-.51	-24.8
12125950	1985	12.55	13.59	1.04	8.3	8.84	9.30	.46	5.2	3.11	3.59	.48	15.4	.36	.46	.10	27.8
	1986	12.25	12.15	-.10	-.8	8.10	8.75	.65	8.0	2.39	1.37	-1.02	-42.7	.56	.57	.01	1.8
12126100	1985	19.24	18.94	-.30	-1.6	11.54	11.36	-.18	-1.6	5.45	5.56	.11	2.0	1.69	1.50	-.19	-11.2
	1986	18.81	17.81	-1.00	-5.3	10.21	10.70	.49	4.8	4.82	4.03	-.79	-16.4	1.95	1.46	-.49	-25.1
12126800	1985	17.94	17.87	-.07	-.4	11.94	10.58	-1.36	-11.4	4.58	4.95	.37	8.1	.58	1.35	.77	132.8
	1986	16.73	16.34	-.39	-2.3	9.25	8.72	-.53	-5.7	3.48	3.40	-.08	-2.3	.84	1.41	.57	67.9
12126900	1985	17.55	17.55	.00	.0	10.43	12.14	1.71	16.4	5.03	5.07	.04	.8	.83	1.39	.56	67.5
	1986	14.95	15.79	.84	5.6	10.55	10.91	.36	3.4	2.97	3.13	.16	5.4	1.05	1.55	.50	47.6
12127100	1985	16.74	19.42	2.68	16.0	11.01	10.81	-.20	-1.8	5.11	5.00	-.11	-2.2	1.15	1.42	.27	23.5
	1986	17.51	18.14	.63	3.6	10.20	9.61	-.59	-5.8	3.68	3.43	-.25	-6.8	1.18	1.46	.28	23.7
12122500	1985	22.00	19.53	-2.47	-11.2	12.43	11.49	-.94	-7.6	6.83	5.69	-1.14	-16.7	1.78	1.63	-.15	-8.4
	1986	21.00	20.10	-.90	-4.3	11.85	12.26	.41	3.5	5.66	5.30	-.36	-6.4	1.94	1.54	-.40	-20.6
12123100	1985	17.59	17.45	-.14	-.8	9.83	10.45	.62	6.3	5.27	5.32	.05	1.0	1.63	1.14	-.49	-30.1
	1986	17.04	17.33	.29	1.7	9.51	11.18	1.67	17.6	4.64	4.00	-.64	-13.8	1.82	1.04	-.78	-42.9
12123200	1985	11.00	8.48	-2.52	-22.9	5.57	5.47	-.10	-1.8	3.44	2.05	-1.39	-40.4	1.36	.70	-.66	-48.5
	1986	10.40	10.71	.31	3.0	5.15	6.83	1.68	32.6	3.22	2.82	-.40	-12.4	1.18	.51	-.67	-56.8

Table 4.--Observed and simulated annual and seasonal runoff data-continued

Station number	Water year	Annual runoff[1] Obs.	Annual runoff[1] Sim.	Annual runoff[1] Difference Inches	Annual runoff[1] Difference Percent	Winter runoff[2] Obs.	Winter runoff[2] Sim.	Winter runoff[2] Difference Inches	Winter runoff[2] Difference Percent	Spring runoff[3] Obs.	Spring runoff[3] Sim.	Spring runoff[3] Difference Inches	Spring runoff[3] Difference Percent	Summer runoff[4] Obs.	Summer runoff[4] Sim.	Summer runoff[4] Difference Inches	Summer runoff[4] Difference Percent
12124000	1985	16.60	16.27	-.33	-2.0	9.21	8.57	-.64	-7.0	5.43	5.69	.26	4.8	1.28	1.42	.14	10.9
	1986	16.33	17.41	1.08	6.6	8.58	10.00	1.42	16.6	4.93	5.00	.07	1.4	1.43	1.29	-.14	-9.8
12124500	1985	16.42	17.10	.68	4.1	8.92	9.90	.98	11.0	5.29	5.22	-.07	-1.3	1.47	1.35	-.12	-8.2
	1986	17.52	17.68	.16	.9	9.35	10.76	1.41	15.1	5.17	4.59	-.58	-11.2	1.70	1.24	-.46	-27.1
12109500	1985	18.93	18.35	-.58	-3.1	9.78	9.74	-.04	-.4	5.54	5.00	-.54	-9.8	2.62	2.68	.06	2.3
	1986	23.79	24.50	.71	3.0	13.69	12.92	-.77	-5.6	6.38	7.18	.80	12.5	2.37	3.00	.63	26.6
12110000	1985	14.34	13.42	-0.92	-6.4	8.42	8.37	-0.05	-0.6	4.27	3.29	-0.98	-23.0	1.10	1.25	0.15	13.6
	1986	19.83	19.91	.08	.4	12.00	11.48	-.52	-4.3	5.49	5.57	.08	1.5	1.33	1.58	.25	18.8
12110400	1985	25.66	25.39	-.27	-1.0	12.05	12.16	.11	.9	9.82	8.64	-1.18	-12.0	2.88	3.73	.85	29.5
	1986	45.81	39.68	-6.13	-13.4	20.00	16.91	-3.09	-15.4	18.45	16.39	-2.06	-11.2	5.28	5.00	-.28	-5.3
12110500	1985	22.03	20.36	-1.67	-7.6	10.75	10.23	-.52	-4.8	7.88	6.61	-1.27	-16.1	2.46	2.75	.29	11.8
	1986	29.49	32.22	2.73	9.3	14.23	14.47	.24	1.7	10.86	12.85	1.99	18.3	3.04	3.70	.66	21.7
12112000	1985	10.41	9.68	-.73	-7.0	5.76	5.75	-.01	-.2	4.12	3.09	-1.03	-25.0	.39	.67	.28	71.8
	1986	16.96	18.05	1.09	6.4	8.60	9.54	.94	10.9	7.64	7.24	-.40	-5.2	.52	.95	.43	82.7
12112550	1986	16.31	17.27	.96	5.9	10.98	10.74	-.24	-2.2	4.04	4.41	.37	9.2	.43	.90	.47	109.3
12112600	1985	15.56	13.90	-1.66	-10.7	8.37	7.96	-.41	-4.9	5.19	4.02	-1.17	-22.5	1.40	1.43	.03	2.1
	1986	22.16	22.06	-.10	-.4	11.72	11.38	-.34	-2.9	7.93	7.87	-.06	-.8	1.62	1.88	.26	16.0

[1] Annual runoff data are the total streamflow volumes for each water year (October-September).

[2] Winter runoff data are the total streamflow volumes for each winter season (November-February).

[3] Spring runoff data are the total streamflow volumes for each spring season (March-June).

[4] Summer runoff data are the total streamflow volumes for each summer season (July-September).

Table 5.--Observed and simulated storm runoff and peak discharge data

[Obs. = Observed value, in inches for runoff and in cubic feet per second for discharges; Sim. = Simulated value, in inches for runoff and in cubic feet per second for discharges; Difference, inches = Sim. - Obs., in inches for runoff and in cubic feet per second for discharges; Difference, percent = 100 x [(Sim. - Obs.)/Obs.], in percent.]

Station number	Date of storm	Date of peak	Storm runoff[1] Obs.	Storm runoff[1] Sim.	Storm runoff[1] Difference Inches	Storm runoff[1] Difference Percent	Peak discharge[2] Obs.	Peak discharge[2] Sim.	Peak discharge[2] Difference Inches	Peak discharge[2] Difference Percent
12157005	12/14-17/84	12/14/84	0.89	0.85	-0.04	-4.49	125.00	141.00	16.00	12.80
	10/26-29/85	10/28/85	.67	.68	.01	1.49	160.00	119.00	-41.00	-25.62
	1/17-21/86	1/19/86	1.31	1.46	.15	11.45	165.00	175.00	10.00	6.06
	4/27-5/1/86	4/29/86	.97	1.02	.05	5.15	135.00	163.00	28.00	20.74
12157020	10/26-29/85	10/28/85	.66	.76	.10	15.15	80.00	77.90	-2.10	-2.63
	1/17-21/86	1/19/86	1.72	1.49	-.23	-13.37	174.00	115.00	-59.00	-33.91
	2/15-18/86	2/16/86	.70	.66	-.04	-5.71	78.00	60.00	-18.00	-23.08
	4/27-5/1/86	4/29/86	1.23	1.04	-.19	-15.45	122.00	106.00	-16.00	-13.11
12125800	12/14-15/84	12/14/84	.44	.48	.04	9.09	58.00	64.90	6.90	11.90
	6/6-8/85	6/7/85	.25	.20	-.05	-20.00	32.00	32.10	0.10	-0.31
	10/26-27/85	10/26/85	.14	.15	.01	7.14	25.00	21.40	-3.60	-14.40
	1/18-19/86	1/18/86	.58	.78	.20	34.48	77.00	83.50	6.50	8.44
12125900	11/23-24/84	11/23/84	.49	.48	-.01	-2.04	189.00	205.00	16.00	8.47
	11/27-28/84	11/27/84	.61	.62	.01	1.64	180.00	166.00	-14.00	-7.78
	12/14-15/84	12/14/84	.68	.69	.01	1.47	247.00	258.00	11.00	4.45
	1/18-19/86	1/18/86	1.30	1.45	.15	11.54	435.00	445.00	10.00	2.30
12125950	2/11-12/85	2/11/85	.29	.32	.03	10.34	29.00	39.00	10.00	34.48
	6/6-8/85	6/7/85	.50	.57	.07	14.00	52.00	47.70	-4.30	-8.27
	10/26-27/85	10/26/85	.42	.43	.01	2.38	153.00	209.00	56.00	36.60
	1/18-19/86	1/18/86	1.58	1.50	-.08	-5.06	51.00	57.80	6.80	13.33
12126100	11/1-2/84	11/2/84	.36	.30	-.06	-16.67	286.00	232.00	-54.00	-18.88
	6/6-8/85	6/7/85	.54	.58	.04	7.41	314.00	298.00	-16.00	-5.10
	10/26-27/85	10/27/85	.46	.40	-.06	-13.04	314.00	248.00	-66.00	-21.02
	1/18-19/86	1/18/86	1.53	1.40	-.13	-8.50	914.00	827.00	-87.00	-9.52
12126800	11/23-24/84	11/23/84	.61	.53	-.08	-13.11	153.00	170.00	17.00	11.11
	11/27-30/84	11/27/84	1.54	1.01	-.53	-34.42	136.00	101.00	-35.00	-25.74
	12/14-15/84	12/14/84	.99	.73	-.26	-26.26	229.00	208.00	-21.00	-9.17
	1/18-19/86	1/18/86	2.22	1.65	-.57	-25.68	439.00	338.00	-101.00	-23.01
12126900	11/23-24/84	11/23/84	.89	.94	.05	5.62	266.00	336.00	70.00	26.32
	12/14-15/84	12/14/84	.66	.76	.10	15.15	147.00	204.00	57.00	38.78
	6/6-8/85	6/7/85	.87	1.00	.13	14.94	176.00	173.00	-3.00	-1.70
	10/26-27/85	10/25/85	.96	.78	-.18	-18.75	189.00	148.00	-41.00	-21.69

Table 5.--Observed and simulated storm runoff and peak discharge data--continued

[Obs. = Observed value, in inches for runoff and in cubic feet per second for discharges; Sim. = Simulated value, in inches for runoff and in cubic feet per second for discharges; Difference, inches = Sim. - Obs., in inches for runoff and in cubic feet per second for discharges; Difference, percent = 100 x [(Sim. - Obs.)/Obs.], in percent.]

Station number	Date of storm	Date of peak	Storm runoff[1] Obs.	Storm runoff[1] Sim.	Storm runoff[1] Difference Inches	Storm runoff[1] Difference Percent	Peak discharge[2] Obs.	Peak discharge[2] Sim.	Peak discharge[2] Difference Inches	Peak discharge[2] Difference Percent
12127100	11/23-24/84	11/23/84	.63	.60	-.03	-4.76	478.00	505.00	27.00	5.65
	11/27-28/84	11/27/84	.65	.58	-.07	-10.77	308.00	289.00	-19.00	-6.17
	12/14-15/84	12/15/84	.73	.66	-.07	-9.59	416.00	434.00	18.00	4.33
	1/18-19/86	1/18/86	2.10	1.62	-.48	-22.86	1,090.00	913.00	-177.00	-16.24
12122500	11/27-12/1/84	11/28/84	1.18	0.88	-0.30	-25.42	147.00	96.90	-50.10	-34.08
	12/14-17/84	12/14/84	1.15	1.09	-.06	-5.22	153.00	138.00	-15.00	-9.80
	6/6-10/85	6/7/85	.96	1.13	.17	17.71	166.00	176.00	10.00	6.02
	1/18-20/86	1/19/86	2.00	2.54	.54	27.00	412.00	504.00	92.00	22.33
12123100	11/27-12/1/84	11/28/84	.87	.88	.01	1.15	88.00	82.10	-5.90	-6.70
	12/14-17/84	12/14/84	.93	1.01	.08	8.60	95.00	108.00	13.00	13.68
	6/6-10/85	6/7/85	.65	.87	.22	33.85	89.00	99.90	10.90	12.25
	1/18-21/86	1/18/86	1.93	2.53	.60	31.09	245.00	320.00	75.00	30.61
12123200	11/28-30/84	11/28/84	.25	.26	.01	4.00	9.30	4.09	-5.21	-56.02
	6/7-8/85	6/7/85	.28	.33	.05	17.86	14.00	8.33	-5.67	-40.50
	10/26-27/85	10/26/85	.12	.14	.02	16.67	11.00	4.09	-6.91	-62.82
	1/18-20/86	1/18/86	.81	1.03	.22	27.16	32.00	34.60	2.60	8.12
12124000	12/8-11/84	12/9/84	.61	.51	-.10	-16.39	74.00	65.20	-8.80	-11.89
	12/12-19/84	12/16/84	1.36	1.02	-.34	-25.00	91.00	66.80	-24.20	-26.59
	6/7-10/84	6/8/84	.92	1.09	.17	18.48	128.00	147.00	19.00	14.84
	10/25-30/85	10/27/85	.76	.66	-.10	-13.16	78.00	65.50	-12.50	-16.03
12124500	11/27-12/1/84	11/29/84	.66	.75	.09	13.64	234.00	286.00	52.00	22.22
	12/7-10/84	12/8/84	.56	.54	-.02	-3.57	232.00	254.00	22.00	9.48
	12/14-17/84	12/15/84	.63	.88	.25	39.68	256.00	375.00	119.00	46.48
	6/7-10/85	6/8/85	.59	1.00	.41	69.49	306.00	502.00	196.00	64.05
12109500	12/7-10/84	12/8/84	.63	.65	.02	3.17	20.00	21.00	1.00	5.00
	12/29/84-1/1/85	12/30/84	.76	.69	-.07	-9.21	24.00	21.90	-2.10	-8.75
	1/18-20/86	1/18/86	1.96	1.51	-.45	-22.96	103.00	70.80	-132.20	-31.26
	2/23-27/86	2/25/86	1.39	1.26	-.13	-9.35	32.00	29.80	-2.20	-6.88
12110000	12/7-10/84	12/8/84	.50	.59	.09	18.00	99.00	113.00	14.00	14.14
	12/29/84-1/1/85	12/30/84	.57	.63	.06	10.53	105.00	113.00	8.00	7.62
	1/18-20/86	1/19/86	1.73	1.33	-.40	-23.12	525.00	368.00	-157.00	29.90
	2/23-27/86	2/25/86	1.13	1.17	.04	3.54	167.00	165.00	-2.00	-1.20

Table 5.--Observed and simulated storm runoff and peak discharge data--continued

[Obs. = Observed value, in inches for runoff and in cubic feet per second for discharges; Sim. = Simulated value, in inches for runoff and in cubic feet per second for discharges; Difference, inches = Sim. - Obs., in inches for runoff and in cubic feet per second for discharges; Difference, percent = 100 x [(Sim. - Obs.)/Obs.], in percent.]

			Storm runoff[1]				Peak discharge[2]			
Station number	Date of storm	Date of peak	Obs.	Sim.	Difference Inches	Difference Percent	Obs.	Sim.	Difference Inches	Difference Percent
12110400	12/29/84-1/1/85	12/30/84	.64	.64	.00	.00	17.00	17.20	.20	1.18
	11/18-19/85	11/18/85	.34	.21	-.13	-38.24	16.00	12.90	-3.10	-19.37
	1/18-19/86	1/19/86	.49	.47	-.02	-4.08	30.00	29.10	-.90	-3.00
	2/23-26/86	2/24/86	1.01	1.01	.00	.00	26.00	26.20	.20	.77
12110500	12/7-11/84	12/8/84	.55	.57	.02	3.64	60.00	56.70	-3.30	-5.50
	12/29/84-1/2/81	2/30/84	.66	.69	.03	4.55	68.00	65.10	-2.90	-4.26
	1/18-21/86	1/19/86	1.01	.88	-.33	-12.87	135.00	115.00	-20.00	-14.81
	2/23-27/86	2/25/86	.97	1.12	.15	15.46	103.00	111.00	8.00	7.77
12112000	12/14-20/84	12/14/84	0.32	0.66	0.34	106.25	46.00	62.10	16.10	35.00
	12/29/84-1/5/85	12/30/84	.67	.71	.04	5.97	52.00	59.40	7.40	14.23
	1/19-27/86	1/23/86	1.54	1.69	.15	9.74	118.00	121.00	3.00	2.54
	2/23-3/3/86	2/26/86	1.58	1.50	-.08	-5.06	132.00	113.00	-19.00	-14.39
12112550	10/27-28/85	10/27/85	.28	.37	.09	32.14	43.00	46.80	3.80	8.84
	1/18-20/86	1/19/86	1.45	1.53	.08	5.52	148.00	172.00	24.00	16.22
	2/23-26/86	2/24/86	1.30	1.12	-.18	-13.85	96.00	60.80	-35.20	-36.67
	3/23-24/86	3/23/86	.17	.20	.03	17.65	31.00	33.20	2.20	7.10
12112600	12/7-10/84	12/8/84	.40	.46	.06	15.00	246.00	277.00	31.00	12.60
	12/29/84-1/2/85	12/30/84	.62	.64	.02	3.23	286.00	289.00	3.00	1.05
	1/18-21/86	1/19/86	1.21	1.11	-.10	-8.26	888.00	725.00	-163.00	-18.36
	2/23-3/1/86	2/25/86	1.34	1.35	.01	.75	468.00	469.00	1.00	.21

[1] Storm runoff data are the total streamflow volumes for the period of each storm.

[2] Peak discharge data are the maximum instantaneous discharges for each storm.

Table 6.--Measures of errors in model-simulated daily mean discharges for each stream-gaging station used for calibration

Station number	Flow regime [1]	Mean absolute error [2]		Root mean square error [3]		Bias [4]		Standard error of estimate [5]	
		Average	Percent	Average	Percent	Average	Percent	Average	Percent
12157005	Low	1.94	23.4	2.36	27.3	-1.44	-18.1	1.87	20.6
	Medium	4.04	22.2	5.30	27.8	-2.00	-11.2	4.94	25.6
	High	7.68	19.9	10.27	26.1	2.43	5.3	10.02	25.6
	Total	4.64	21.8	6.98	27.0	-.16	-7.6	6.98	25.9
12157020	Low	.88	34.0	1.52	49.8	-.26	-12.5	1.50	48.4
	Medium	3.47	39.1	4.56	50.4	-.30	-2.0	4.57	50.5
	High	7.46	37.0	9.79	48.0	3.85	19.8	9.04	43.9
	Total	3.86	36.6	6.21	49.4	1.05	1.4	6.12	49.4
12125800	Low	.48	35.4	.62	41.4	-.27	-21.1	.56	35.7
	Medium	1.03	26.7	1.37	34.7	-.19	-4.5	1.36	34.6
	High	2.93	25.1	4.60	33.0	1.73	10.4	4.28	31.4
	Total	1.45	29.1	2.74	36.5	.39	-5.3	2.71	36.2
12125900	Low	2.44	33.3	2.72	36.2	-2.13	-28.9	1.71	21.8
	Medium	3.46	25.2	4.75	35.1	-.41	-3.7	4.75	35.0
	High	7.85	22.5	11.32	31.4	5.12	13.2	10.14	28.6
	Total	4.61	26.8	7.30	34.3	.90	-6.0	7.24	33.7
12125950	Low	.13	42.5	.26	63.7	.09	31.6	.24	55.5
	Medium	.99	53.6	1.53	82.2	.13	8.7	1.53	82.1
	High	2.89	37.9	4.34	55.4	1.41	17.3	4.12	52.9
	Total	1.33	44.7	2.64	68.2	.54	19.2	2.59	65.4
12126100	Low	3.25	24.3	3.99	28.7	-2.58	-19.9	3.05	20.7
	Medium	6.06	22.4	7.78	28.1	-2.04	-7.8	7.54	27.2
	High	11.66	17.5	17.02	24.3	.08	1.4	17.08	24.3
	Total	7.11	21.3	11.36	27.0	-1.45	-8.8	11.26	25.0
12126800	Low	1.29	87.7	1.56	105.1	1.28	87.2	.91	58.8
	Medium	1.98	37.4	3.14	67.6	.59	17.5	3.09	65.6
	High	5.29	20.9	11.34	29.5	-1.09	2.0	11.34	29.5
	Total	2.84	49.1	6.82	74.5	.27	36.2	6.82	65.2
12126850	Low	.52	45.9	.64	57.8	.40	39.5	.50	42.4
	Medium	1.94	45.9	3.87	91.2	.64	16.4	3.83	90.2
	High	7.01	35.0	20.07	54.5	1.51	17.3	20.09	51.8
	Total	3.17	42.2	11.96	68.5	.85	25.0	11.93	63.8
12127100	Low	1.64	22.8	2.08	26.8	.77	12.2	1.94	24.0
	Medium	4.42	25.9	6.60	39.3	-.41	-1.5	6.62	39.4
	High	9.97	18.2	20.36	24.9	-1.41	-1.0	20.38	25.0
	Total	5.57	22.0	12.99	30.4	-.39	3.2	12.99	30.3

Table 6.--Measures of errors in model-simulated daily mean discharges for each stream-gaging station used for calibration--continued

Station number	Flow regime[1]	Mean absolute error[2]		Root mean Square error[3]		Bias[4]		Standard error of estimate[5]	
		Average	Percent	Average	Percent	Average	Percent	Average	Percent
12122500	Low	1.59	18.6	2.20	23.8	-0.68	-6.2	2.10	23.1
	Medium	4.16	23.5	5.02	28.7	-2.24	-13.0	4.50	25.7
	High	9.37	21.4	14.52	25.7	-2.65	-8.8	14.34	24.3
	Total	4.86	21.1	8.71	26.1	-1.81	-9.2	8.52	24.4
12123100	Low	2.27	35.6	2.49	38.2	-2.10	-30.9	1.33	22.7
	Medium	2.81	22.6	3.56	28.4	-1.01	-10.0	3.43	26.6
	High	6.31	19.8	10.70	25.5	4.18	12.1	9.90	22.6
	Total	3.59	25.9	6.20	31.1	.07	-10.5	6.20	29.3
12123200	Low	.23	48.4	.30	59.1	-.20	-41.6	.23	42.1
	Medium	.40	48.5	.45	55.0	-.23	-29.3	.39	46.7
	High	.73	46.1	1.00	60.0	.09	4.0	1.00	60.1
	Total	.46	47.6	.67	58.2	-.11	-21.5	.66	54.0
12124000	Low	1.18	18.9	1.46	22.6	-.27	-3.1	1.45	22.5
	Medium	2.50	18.8	3.56	26.4	-.52	-3.5	3.54	26.2
	High	7.33	21.0	14.18	27.6	1.71	4.8	14.12	27.3
	Total	3.90	19.6	8.96	25.7	.40	-.2	8.95	25.7
12124500	Low	4.46	18.8	5.40	22.3	-3.35	-14.1	4.24	17.4
	Medium	9.60	18.7	11.89	22.9	-4.66	-9.7	10.98	20.9
	High	26.45	19.1	51.95	24.8	13.62	5.0	50.35	24.4
	Total	13.28	18.9	30.44	23.4	1.67	-6.4	30.39	22.5
12109500	Low	.39	20.2	.47	25.1	.37	19.1	.29	16.4
	Medium	.59	17.4	.90	25.1	.19	5.8	.88	24.6
	High	1.82	21.0	3.02	28.0	-.51	-2.0	2.99	28.1
	Total	.93	19.6	1.83	26.1	.02	7.9	1.83	24.9
12110000	Low	1.55	23.6	1.93	28.7	.78	13.7	1.77	25.4
	Medium	3.09	18.2	4.04	23.4	-1.10	-5.2	3.91	22.9
	High	10.78	23.5	18.17	30.1	-1.53	-.8	18.18	30.2
	Total	5.15	21.9	10.85	27.6	-.60	2.8	10.83	27.5
12110400	Low	.89	27.7	1.07	35.5	.29	13.6	1.03	32.9
	Medium	1.24	14.7	1.53	18.0	-.83	-9.7	1.30	15.2
	High	2.77	18.7	3.33	22.7	-2.24	-15.3	2.48	16.8
	Total	1.63	20.3	2.20	26.3	-.93	-3.9	2.00	26.1
12110500	Low	2.71	21.8	3.05	25.0	1.02	9.5	2.88	23.1
	Medium	3.92	14.7	4.40	16.6	-1.46	-5.1	4.17	15.9
	High	6.81	14.3	8.30	17.1	1.53	3.0	8.18	16.9
	Total	4.62	17.0	5.91	20.0	.53	3.0	5.88	19.8

Table 6.--Measures of errors in model-simulated daily mean discharges for each stream-gaging station used for calibration--continued

Station number	Flow regime[1]	Mean absolute error[2]		Root mean square error[3]		Bias[4]		Standard error of estimate[5]	
		Average	Percent	Average	Percent	Average	Percent	Average	Percent
12112000	Low	1.76	69.0	1.98	75.5	1.75	68.8	0.92	31.3
	Medium	4.35	29.0	5.50	36.3	-.92	-2.9	5.44	36.3
	High	9.46	24.1	10.97	28.6	.03	.7	11.01	28.8
	Total	5.18	40.7	7.16	51.2	.29	22.3	7.16	46.1
12112550	Low	.69	97.0	.78	107.6	.63	91.2	.48	57.4
	Medium	1.04	28.2	1.57	44.6	.33	10.0	1.55	43.9
	High	4.11	35.4	5.98	49.8	.20	7.7	6.02	49.6
	Total	2.05	54.8	3.75	74.2	.39	37.4	3.74	64.3
12112600	Low	5.07	17.1	6.17	20.9	.44	2.8	6.18	20.8
	Medium	13.65	16.9	17.73	20.6	-6.35	-8.1	16.62	19.0
	High	24.17	15.2	30.49	18.3	-7.46	-4.1	29.69	17.9
	Total	13.94	16.4	20.25	20.0	-4.34	-3.1	19.78	19.8

[1] Low, medium, and high flow regimes are the lower, middle, and upper thirds of the flow duration curve of daily mean discharge values from each station. Total refers to the complete daily mean flow record at the station.

[2] S = simulated daily mean discharge, in cubic feet per second.
O = Observed daily mean discharge, in cubic feet per second.
N = number of daily values in the sample.
Mean absolute error, average = $\Sigma[(S-O) /N]$.
Mean absolute error, percent = $100 \times \Sigma\{[(S-O) /O]/N\}$.

[3] Root mean square error, average = $\sqrt{\Sigma[(S-O)^2/N]}$.

Root mean square error, percent = $100 \times \sqrt{\Sigma[(S-O/O)^2/N]}$.

[4] Bias, average = $\Sigma[(S-O)/N]$.
Bias, percent = $100 \times \Sigma\{[(S-O)/O]/N\}$.

[5] Standard error of estimate, average =

$$[N/(N-1)] \times \sqrt{(\text{Root mean square error, average})^2 - (\text{Bias, average})^2}.$$

Standard error of estimate, percent =

$$[N/(N-1)] \times \sqrt{(\text{Root mean square error, percent})^2 - (\text{Bias, percent})^2}.$$

Table 7.--Measures of composite errors in model-simulated annual runoff, seasonal runoff, storm runoff, peak discharges, and daily mean discharges simulated for all stream gages and basins with the regionally calibrated model

	Mean absolute error [1]		Root mean square error [2]		Bias [3]		Standard error of estimate [4]	
Data set name	Average	Percent	Average	Percent	Average	Percent	Average	Percent
Annual runoff	1.03	5.6	1.53	7.7	0.01	-0.5	1.53	7.9
Winter runoff	.81	8.4	1.08	11.7	-.29	-4.3	1.08	11.2
Spring runoff	.53	9.9	.75	13.9	.27	5.5	.75	13.1
Summer runoff	.36	31.0	.42	42.1	-.02	-9.1	.42	40.1
Storm runoff	.13	15.0	.19	21.3	.01	-2.9	.19	21.4
Peak discharge	29.24	16.4	50.19	21.5	3.03	1.4	50.19	21.7
Daily mean discharge								
Low flow	1.71	35.0	2.61	48.4	-.28	7.5	2.59	47.9
Medium flow	3.62	27.1	6.22	43.0	-1.13	-3.7	6.12	42.8
High flow	8.25	24.2	17.35	34.5	.98	4.2	17.33	34.3
Total	4.54	28.8	10.80	42.4	-.13	2.8	10.80	42.3

[1] S = simulated daily mean discharge, in cubic feet per second.
O = Observed daily mean discharge, in cubic feet per second.
N = number of daily values in the sample.
Mean absolute error, average = $\Sigma[\ (S-O)\ /N)]$.
Mean absolute error, percent = $100 \times \Sigma\{[\ (S-O)\ /O]/N\}$.

[2] Root mean square error, average = $\sqrt{\Sigma[(S-O)^2/N]}$.

Root mean square error, percent = $100 \times \sqrt{\Sigma[(S-O/O)^2/N]}$.

[3] Bias, average = $\Sigma[(S-O)/N]$.
Bias, percent = $100 \times \Sigma\{[(S-O)/O]/N\}$.

[4] Standard error of estimate, average =

$$[N/(N-1)] \times \sqrt{[(\text{Root mean square error, average})^2 - (\text{Bias, average})^2]}.$$

Standard error of estimate, percent =

$$[N/(N-1)] \times \sqrt{[(\text{Root mean square error, percent})^2 - (\text{Bias, percent})^2]}.$$

[5] Low, medium, and high flow regimes are the lower, middle, and upper thirds of the flow duration curve of daily mean discharge values from each station. Total refers to the complete 2-year record of daily mean flow at the station.

Analysis of Errors in the Simulation Model

The errors reported from runoff simulation with the regional model come from two distinct sources: inadequate or inaccurate rainfall, streamflow, and PET data; and inadequate representation of the region's rainfall-runoff relations by the model. Although the large-frontal-system storms that generate large amounts of runoff in the Puget Sound area are commonly assumed to be relatively homogeneous throughout the region, the data collected for this study show that rainfall can have substantial areal variation. Local small-scale variations in rainfall amounts and intensities do exist in the study basins, and it is doubtful that only one rain gage per 10 mi^2 is adequate to represent this variation. Also, the rainfall gages do not adequately measure precipitation as snowfall. Although snow is not common in the study region, about 6 inches of snow was recorded at SEATAC in February 1985, and another 18 inches was recorded in November 1985. Periods of snow accumulation and occasional gage malfunctions resulted in a loss of about 12 percent of the rainfall record for all stations combined. Rainfall for periods of missing record was estimated from data from nearby operating stations because continuous records are required for model calibration, but estimating obviously introduces some amount of error.

Streamflow data were not subject to the same spatial and temporal errors as precipitation, but these data are subject to other sources of error. The stream-gaging stations were operated at sites chosen for model-calibration purposes. Most of those sites had unstable channels and stage-discharge relations that varied during the period of record. Frequent current-meter measurements were made to try to keep these relations as accurate as possible, but most streamflow records used for model calibration were rated "fair," or within 15 percent of their true values 95 percent of the time. Frozen gages and other malfunctions resulted in a loss of about 9 percent of the total streamflow records, which were subsequently estimated by comparison with records and hydrographs for gages in similar nearby basins.

Daily rates of PET for the entire study region were derived from pan evaporation data for Puyallup, Washington, and from temperature data for SEATAC. Actual PET rates vary somewhat among and within drainage basins, so this is another likely source of errors.

Although it is not possible to assign accurate magnitudes to all the errors in the basic data, the errors do exist and they do have an effect on the simulation accuracy of the model. With this in perspective, the overall validity of the simulation model and the hypothesized rainfall-runoff relations on a basin-wide scale are discussed in the following sections.

Annual and Seasonal Runoff

Data in tables 4 and 7 show that the simulation of annual runoff was generally unbiased for the region as a whole, and that errors in annual runoff ranged from 0 to 23 percent at individual gaging stations with a regional standard error of estimate of 8 percent. Simulated winter and spring runoff show a small negative and positive bias, respectively, and had standard errors of estimate of 11 and 13 percent. Summer runoff simulation showed a negative bias of 9 percent and a standard error of estimate of 40 percent. The relatively small errors in the simulation of annual, winter, and spring runoff are well within the limitations of the observed data, and do not suggest any significant model inadequacies in representing regional water balances during most of the year. The much larger simulation errors for summer runoff do suggest that stream baseflow characteristics are not being properly represented. A closer inspection of the segmentation scheme used for this model and of the ground-water systems in the study region provides insight into model inadequacies with respect to simulating summer flows.

The soils, surficial geology, and topography of the study area were some of the primary considerations in developing the segmentation scheme for the model because of the consistent relation between surficial physiography and storm-runoff generation. However, the amount and timing of ground-water discharge that produces baseflow in the upland streams are probably related more to geologic stratigraphy than to the surficial characteristics of the region. The stratigraphy of the region is under investigation, and a detailed analysis of the stratigraphy and the ground-water hydraulics may some day provide information that will help to simulate more adequately the subtleties of summer runoff in these basins.

Storm Runoff and Peak Discharge

Data in tables 5 and 7 show that the simulation values of large storm runoff volumes and peak discharges were unbiased for the region as a whole. Errors for individual events ranged from 0 to 106 percent for runoff volumes, but only 2 of 84 runoff volumes were in error more than 40 percent. Errors for peak discharges ranged from less than 1 to 64 percent, but only 3 of 84 peak discharges were in error more than 40 percent. The standard errors of estimate for storm runoff volumes and peaks were 21 and 22 percent, respectively. The magnitude of these errors does not suggest that any significant model inadequacies exist for the study area as a whole, but rather that some specific storm events in some basins were poorly simulated.

The previously mentioned sources of error in annual and seasonal runoff simulation also affect storm-runoff simulation. There were no obvious correlations between any one segment type and simulation errors that may be attributed to that segment type. Subsequent validation of the model in additional basins may provide more information on errors associated with specific land segments.

Daily Mean Discharge

Data in tables 6 and 7 show that the simulation of daily mean low-flow discharge had an 8-percent positive bias, but the simulation of medium, high, and combined total daily mean discharges had a much smaller bias. The standard error of estimate for the totals of all daily mean flows at individual stations ranged from 20 to 65 percent, and was 42 percent for the region as a whole. All of the previously mentioned sources of error probably apply to the simulation of daily mean flows. The magnitude of the daily flow simulation errors does not suggest any inadequacies in the model. The regional standard errors of estimate for low, medium, and high daily flows were 48, 43, and 34 percent respectively, again reflecting that the model performs best while simulating high flows, and is least accurate when simulating low flows.

In summary, the simulation errors that remained after model calibration were not serious enough to reject the formulated hypotheses concerning rainfall-runoff relations in the study area. The postulated mechanisms of storm-runoff generation appeared to be well supported by the simulation model results, although interstorm and dry-period streamflow generation were not as well represented.

SUMMARY

The purpose of this study was to characterize and simulate rainfall-runoff relations in five headwater drainage basins in western King and Snohomish Counties, Washington. Local planners and engineers need this information in order to minimize the hydrologic impact of urbanization in these basins.

The characteristics of rainfall-runoff relations were hypothesized for the study area as a whole, using existing information. In undisturbed areas, Horton overland flow, runoff generated from rain falling at a greater rate than the infiltration rate of the soil, is not a significant mechanism. Shallow-subsurface flow from hillslopes mantled with glacial till, ground-water flow from glacial outwash deposits, and saturation overland flow from depressions, stream bottoms, and till-capped hilltops are the significant runoff mechanisms. In disturbed, primarily urbanized areas, Horton overland flow is a significant mechanism, along with overland flow from impervious surfaces.

These hypothesized characteristics were incorporated into the Hydrologic Simulation Program-FORTRAN (HSPF) simulation model, and the model was calibrated concurrently at 21 stream-gage sites in the study area. Hydrologic data from the 1985-86 water years were used in this effort. The calibration resulted in 12 sets of generalized HSPF parameters, one set for each land-segment type with a unique hydrologic response. The generalized parameters can be used with HSPF to simulate runoff from most headwater basins within the study area.

The average standard errors of estimate for calibrated streamflow simulation at all 21 sites were 7.9 percent for annual runoff, 11.2 percent for winter runoff, 13.1 percent for spring runoff, 40.1 percent for summer runoff, 21.7 percent for storm peak discharge, 21.4 percent for storm runoff volume, and 42.3 percent for all daily mean discharges. High flows were simulated more accurately than were low flows.

The simulation errors were not large enough to reject the hypothesized rainfall-runoff relations. The simulation model will be validated at 12 additional stream-gage sites in a different set of drainage basins in the same physiographic region.

REFERENCES CITED

Alley, William A., and Veenhuis, Jack E., 1983, Effective impervious area in urban runoff modeling: Journal of Hydrological Engineering, ASCE, v. 109, no. 2, February 1983, p. 313-319.

Bauer, H.H., and Vaccaro, J.J., 1986, Documentation of a deep percolation model for estimating ground-water recharge: U.S. Geological Survey Open-File Report 86-536, 180 p.

Crandell, Dwight R., Mullineaux, Donal R., and Waldron, Howard H., 1965, Age and origin of the Puget Sound trough in western Washington: U.S. Geological Survey Professional Paper 525-B, p. B132-B136.

Dunne, Thomas, and Black, Richard D., 1970, An experimental investigation of runoff production in permeable soils: Water-Resources Research, v. 6, no. 2, p. 478-490.

Farnsworth, Richard K., and Thompson, Edwin S., 1982, Mean monthly, seasonal, and annual pan evaporation for the United States: National Oceanographic and Atmospheric Administration Technical Report NWS 34, U.S. Department of Commerce, Office of Hydrology, National Weather Service, 82 p.

Laenen, Antonius, 1983, Storm runoff as related to urbanization based on data collected in Salem and Portland, and generalized for the Williamette Valley, Oregon: U.S. Geological Survey Water-Resources Investigations Report 83-4143, 88 p.

Leavesley, George H., Lichty, Robert W., Troutman, Brent M., and Saludon, Linda G., 1983, Precipitation-runoff modeling system: U.S. Geological Survey Water-Resources Investigations Report 83-4238, 9 p.

Liesch, Bruce A., Price, Charles E., and Walters, Kenneth L., 1963, Geology and ground-water resources of northwestern King County, Washington: State of Washington Department of Conservation Water-Supply Bulletin No. 20, 241 p.

Luzier, James E., 1969, Geology and ground-water resources of southwestern King County, Washington: State of Washington Department of Water Resources Water-Supply Bulletin No. 28, 260 p.

Newcomb, Robert C., 1952, Ground-water resources of Snohomish County, Washington: U.S. Geological Survey Water-Supply Paper 1135, 133 p.

Pearce, A.J., Stewart, M.K., and Sklash, M.G., 1986, Storm runoff generation in humid headwater catchments 1. where does the water come from?: Water-Resources Research, v. 22, no. 8, p. 1263-1272.

Prych, Edmund A., and Ebbert, J.C., 1986, Quantity and quality of storm runoff from three urban catchments in Bellevue, Washington: U.S. Geological Survey Water-Resources Investigations Report 86-4000, 85 p.

Savini, John, and Kammerer, J.C., 1961, Urban growth and the water regimen: U.S. Geological Survey Water-Supply Paper 1591-A, p. A5-A8.

Snider, M.D., and Miller, R.F., 1985, Effects of tractor logging on soils and vegetation in eastern Oregon: Soil Science Society of America Journal, v. 49, p. 1280-1282.

U.S. Department of Agriculture, 1973, Soil survey of King County area, Washington: U.S. Department of Agriculture Soil Conservation Service, 100 p.

-----1983, Soil survey of Snohomish County area, Washington: U.S. Department of Agriculture Soil Conservation Service, 197 p.

U.S. Department of Commerce, 1973, Precipitation-frequency atlas of the western United States, Volume IX-Washington: NOAA Atlas 2, National Oceanographic and Atmospheric Administration, National Weather Service, Silver Spring, Maryland, 43 p.

-----1982, Monthly normals of temperature, precipitation, and heating and cooling degree days 1951-80, Washington: Climatography of the United States no. 81, 17 p.

U.S. Environmental Protection Agency, 1984, Hydrologic simulation program-FORTRAN (HSPF): Users manual for release 8.0: EPA-600/3-84-066, Environmental research, 767 p.

U.S. Geological Survey, 1988, Water resources data, Washington, water year 1986: U.S. Geological Survey Water-Data Report WA-86-1, 517 p.

U.S. Weather Bureau, 1965, Mean annual precipitation, 1930-1957, State of Washington: Portland, Oregon, U.S. Soil Conservation Service Map M-4430.

GPO 794-363/23064